
SDO/AIA- 193 20100803_120420

Spectral Observations and Radiative Transfer

Mihalis Mathioudakis

Physics and Astronomy, Queen's University Belfast

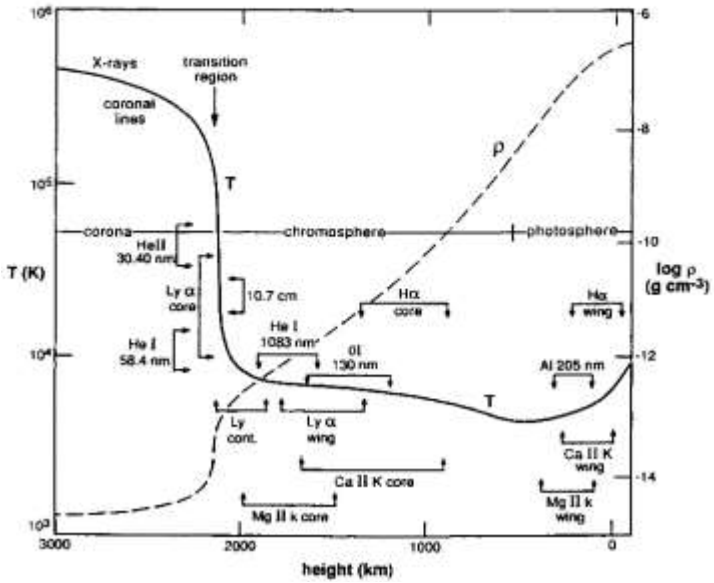

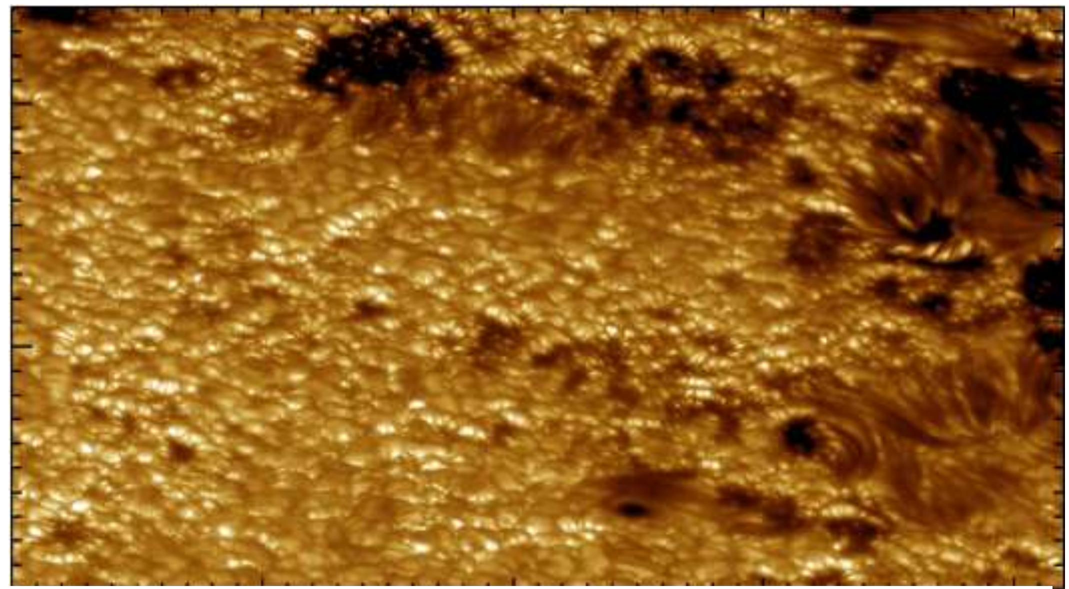

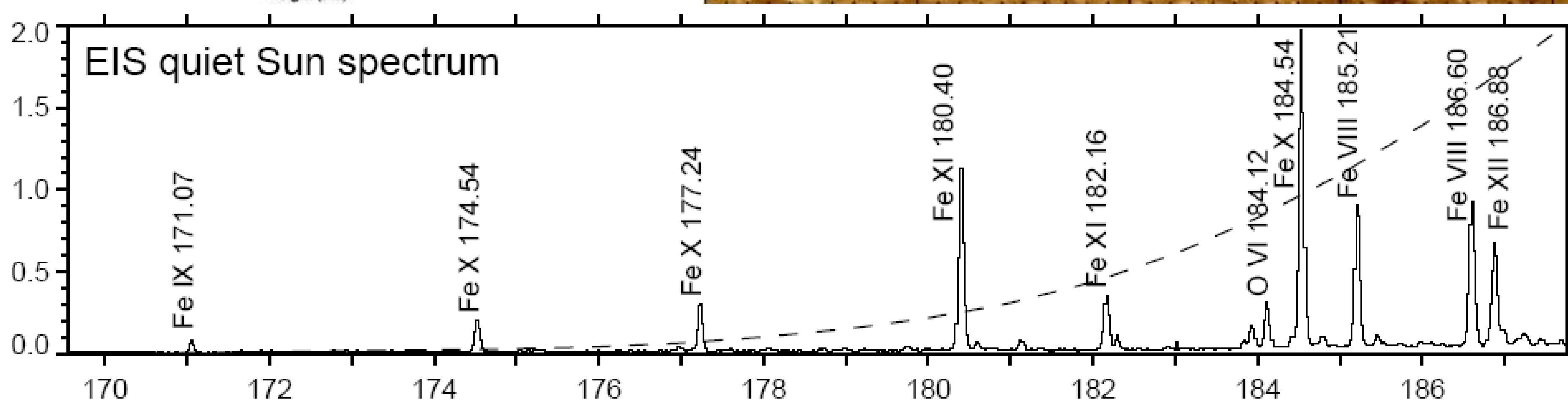

Lecture Outline

- Optically thick emission – Photosphere and Chromosphere
- Radiative transfer equation – LTE & non-LTE
- Optically thin emission – Transition Region & Corona
- Formation of emission and absorption lines
- Line profiles and Line fluxes
- Physical properties from line profiles
- Astronomical techniques

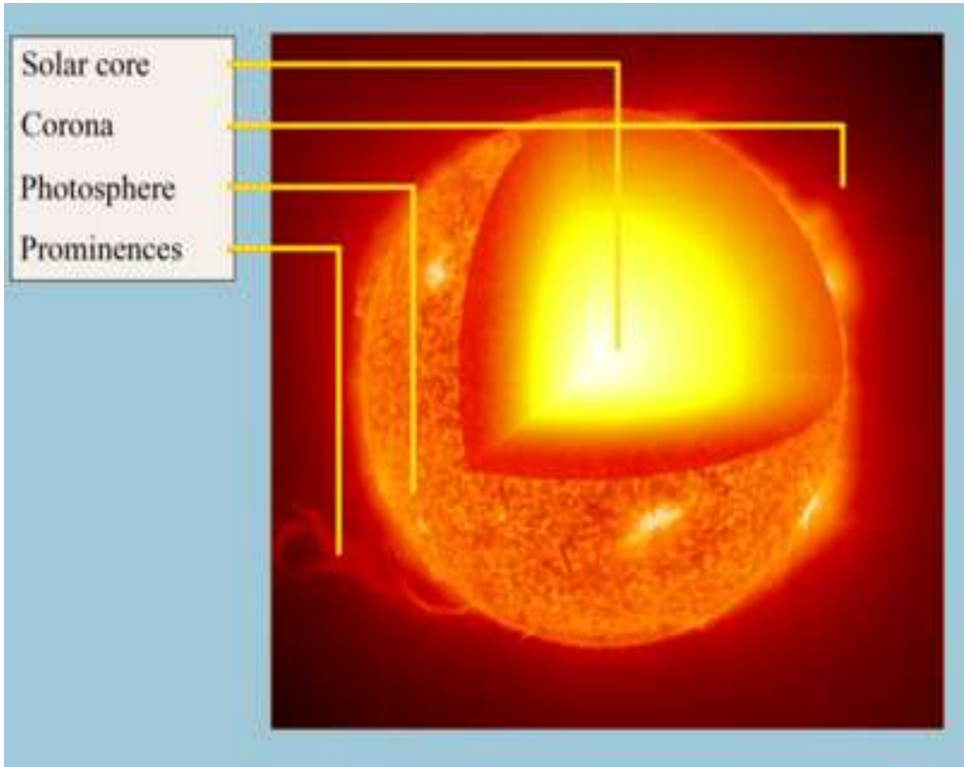

Evolution of our understanding (Schrijver)

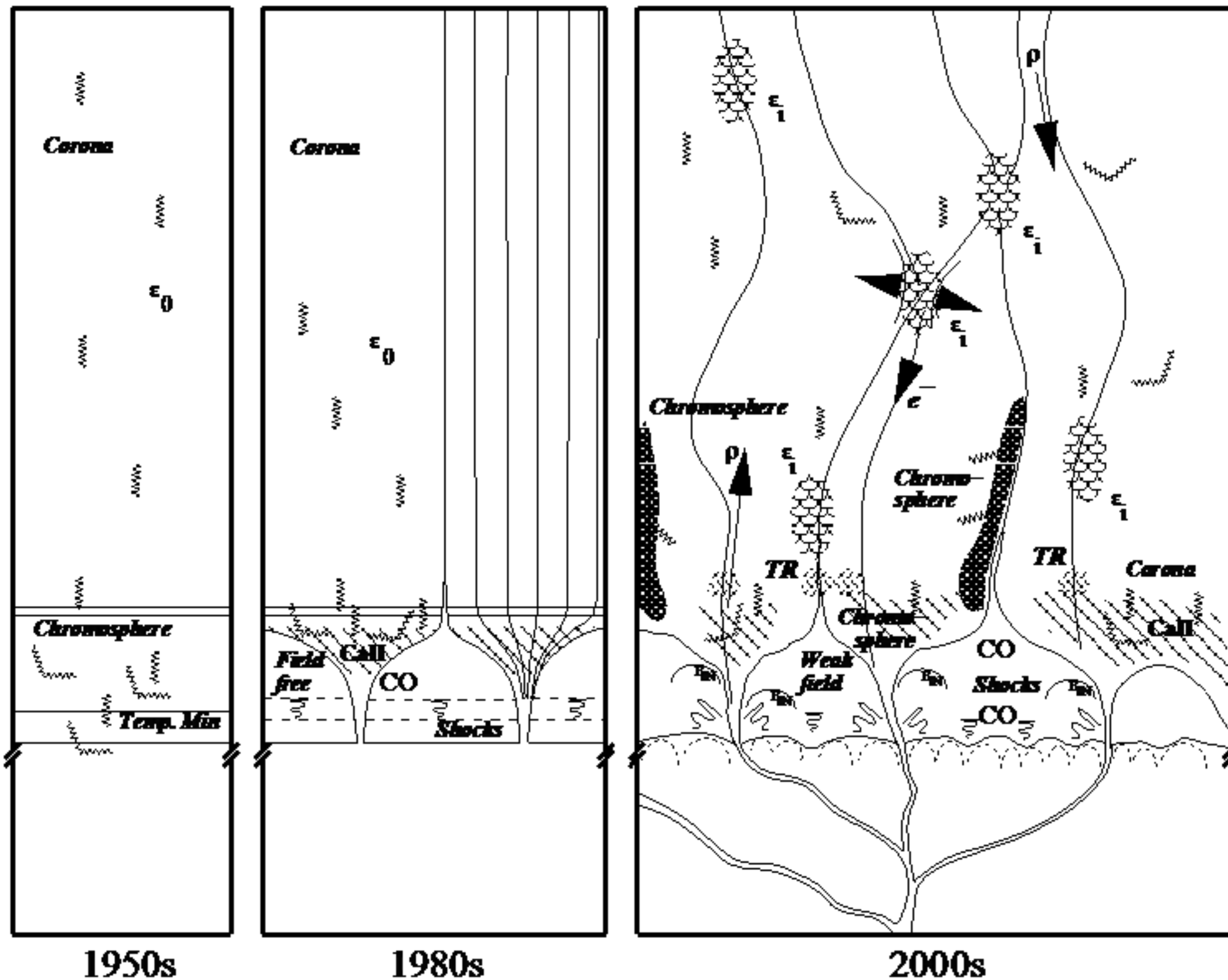

Constructing a physical model.

What observational parameters do you need?

- Intensity maps

  Spatial information (horizontal & vertical)

- Doppler maps

  Velocity information (horizontal & vertical)

- Magnetic field

  Strength & direction

VAL Model

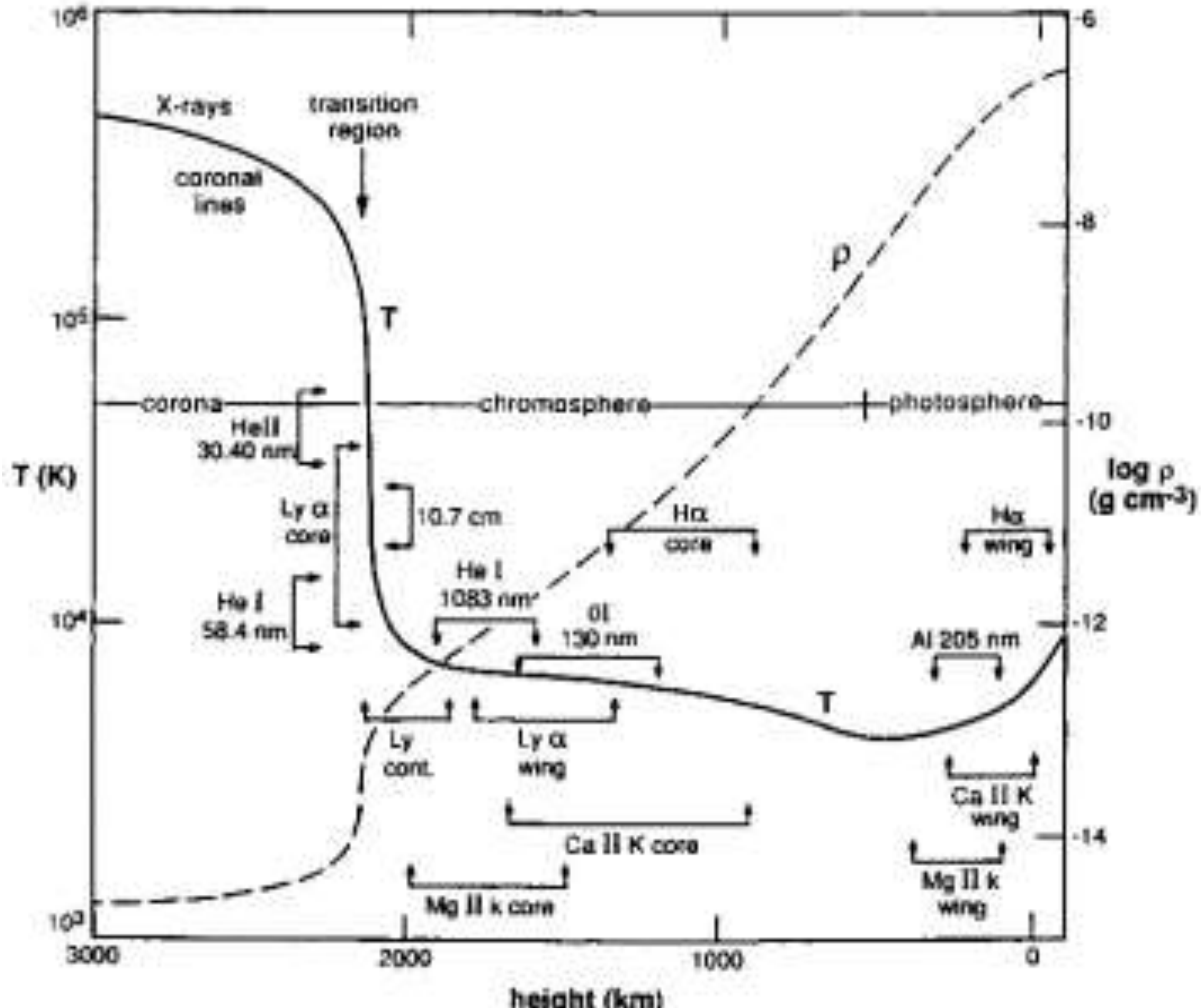

Vernazza et al. (1976, 1981)

Photosphere - The "skin"

- Emits 99% of the energy generated in the interior

- Temperature decreases with height
  6000 K > T > 4000 K

- Density 0.0002 g/cm^{-3}
  6 times less dense than air

- $\beta > 1$ (gas pressure/magnetic pressure)
  $\beta < 1$ in magnetic areas

- Mass of the solar atmosphere ≈ Mass of the photosphere

- Deep in the photosphere TE can apply
  ($I_\lambda = B_\lambda(T)$, Boltzmann & Saha equations apply)

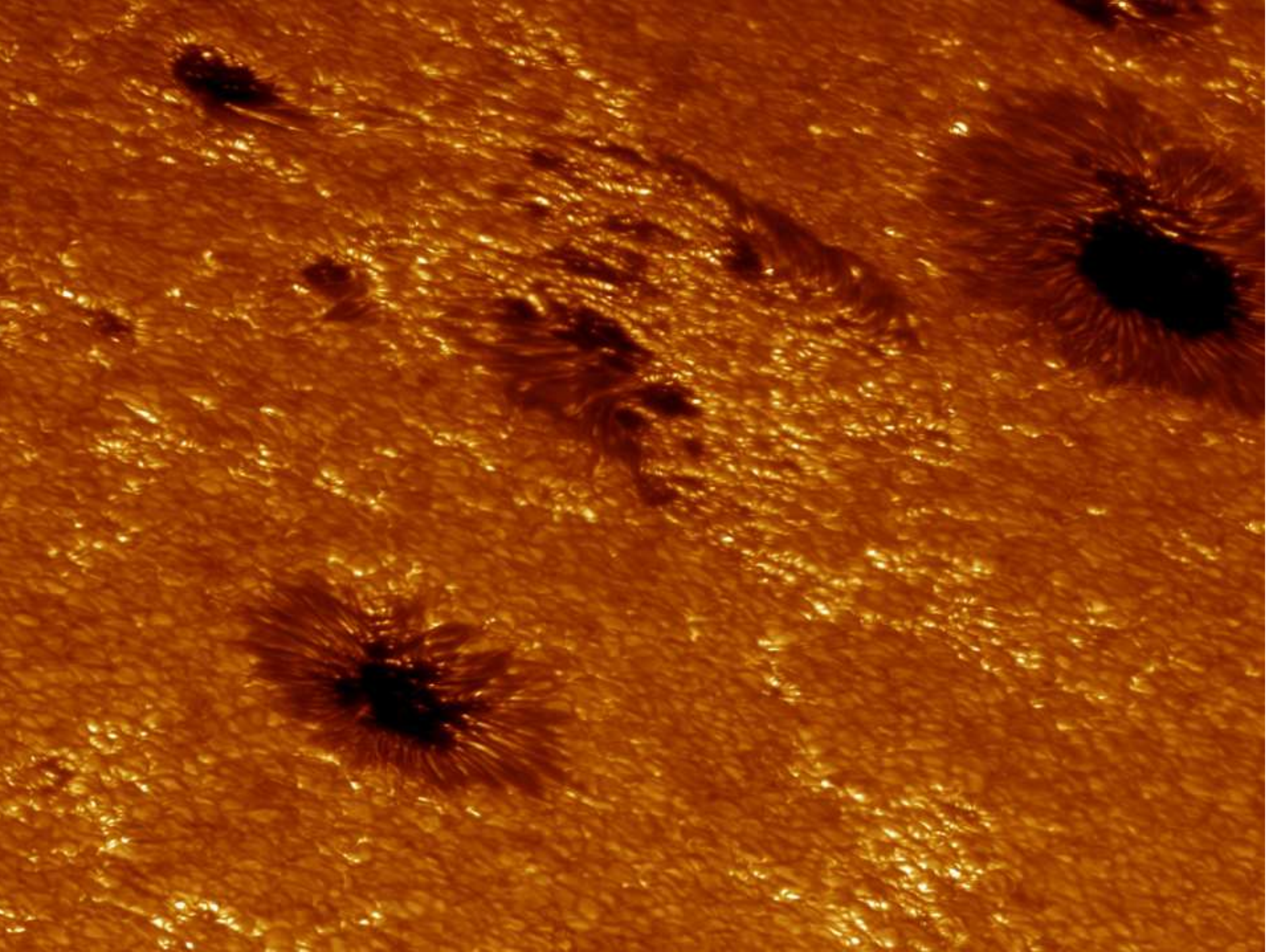

Hydrostatic Equilibrium

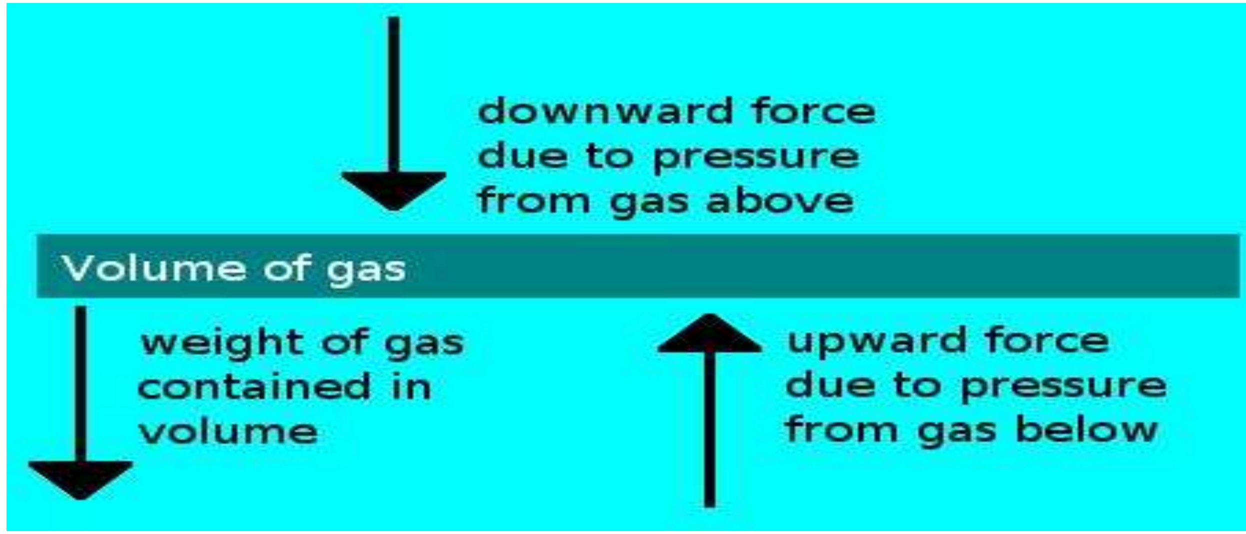

- Upwards pressure force = downward pressure force + gravity
- $dP = \rho\, g\, dx$
- $P = P_o\, e^{-(x/H)}$ $H = KT/g\,m$ (scale height)
- The pressure (density) drops with height

Statistical Equilibrium

Transitions up

- Radiative Excitation – $N_{12} = n_1 B_{12} J_{12}$
- Collisional Excitation – $N'_{12} = n_{12} n_e C_{12}$

Transitions down

- Radiative de-Excitation – $N_{21} = n_2 A_{21}$ (spontaneous emission)
- Collisional de-Excitation – $N_{21}' = n_2 n_e C_{21}$

In Equilibrium: $n_1 B_{12} J_{12} + n_{12} n_e C_{12} = n_2 A_{21} + n_2 n_e C_{21}$

Radiative transfer equation

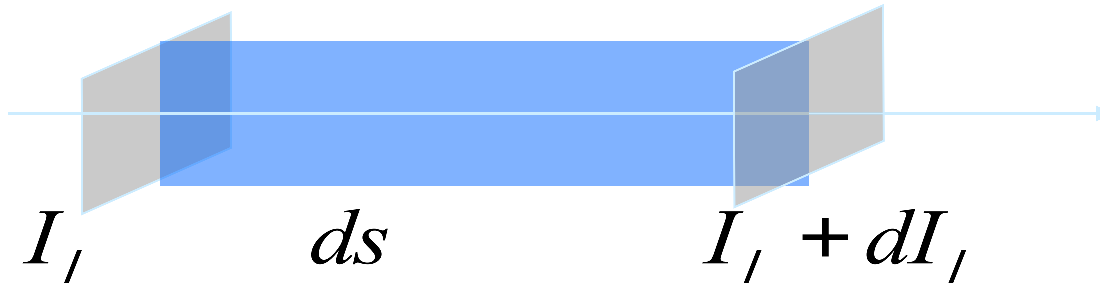

- $$\frac{dI_\lambda}{k_\lambda \rho ds} = - I_\lambda + S_\lambda$$
- $d\tau_\lambda = k_\lambda \, \rho \, ds$
- Intensity reduced by absorption and increased by emission
- k_λ - Absorption Coefficient
- $S_\lambda = \frac{j_\lambda}{k_\lambda}$ Source function (emission/absorption)
- Emission and absorption coefficients depend on the physical parameters of the atmosphere (T, P, abundance) and atomic data of the transitions involved

RT equation: Solution

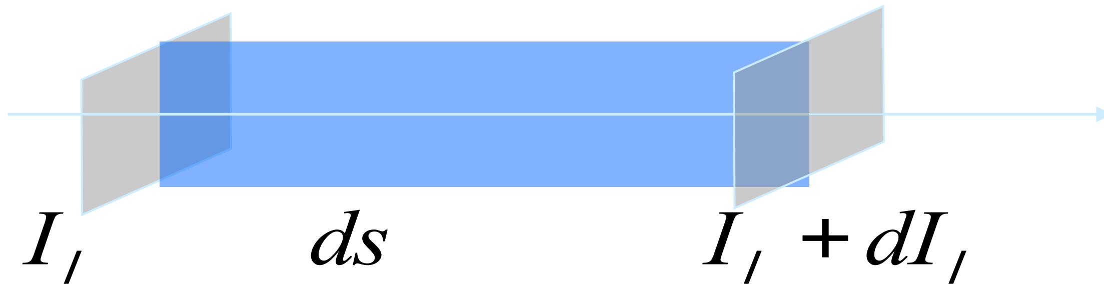

- $I_\lambda(\tau_\lambda) = I_\lambda(0)e^{-\tau_\lambda} + \int_0^{\tau_\lambda} S_\lambda \, e^{(t_\lambda - \tau_\lambda)} \, d t_\lambda$

Special Cases

Pure Absorption : $I_\lambda(\tau_\lambda) = I_\lambda(0)e^{-\tau_\lambda}$

Pure Emission : $I_\lambda(\tau_\lambda) = I_\lambda(0) + \int_0^{s} j_\lambda \, \rho \, ds$

Vacuum : $I_\lambda(\tau_\lambda) = I_\lambda(0)$

LTE versus non-LTE

- Local Thermodynamic Equilibrium

  Level populations dominated by collisions – High density

  Boltzmann statistics/equation can be used

  The source function (S_λ) is equal to the Planck function (B_λ)

- Non-Local Thermodynamic Equilibrium

  Level populations are affected by the radiation field. That radiation field is not necessarily generated locally

  Scattering of radiation becomes important

  Boltzmann statistics no longer apply

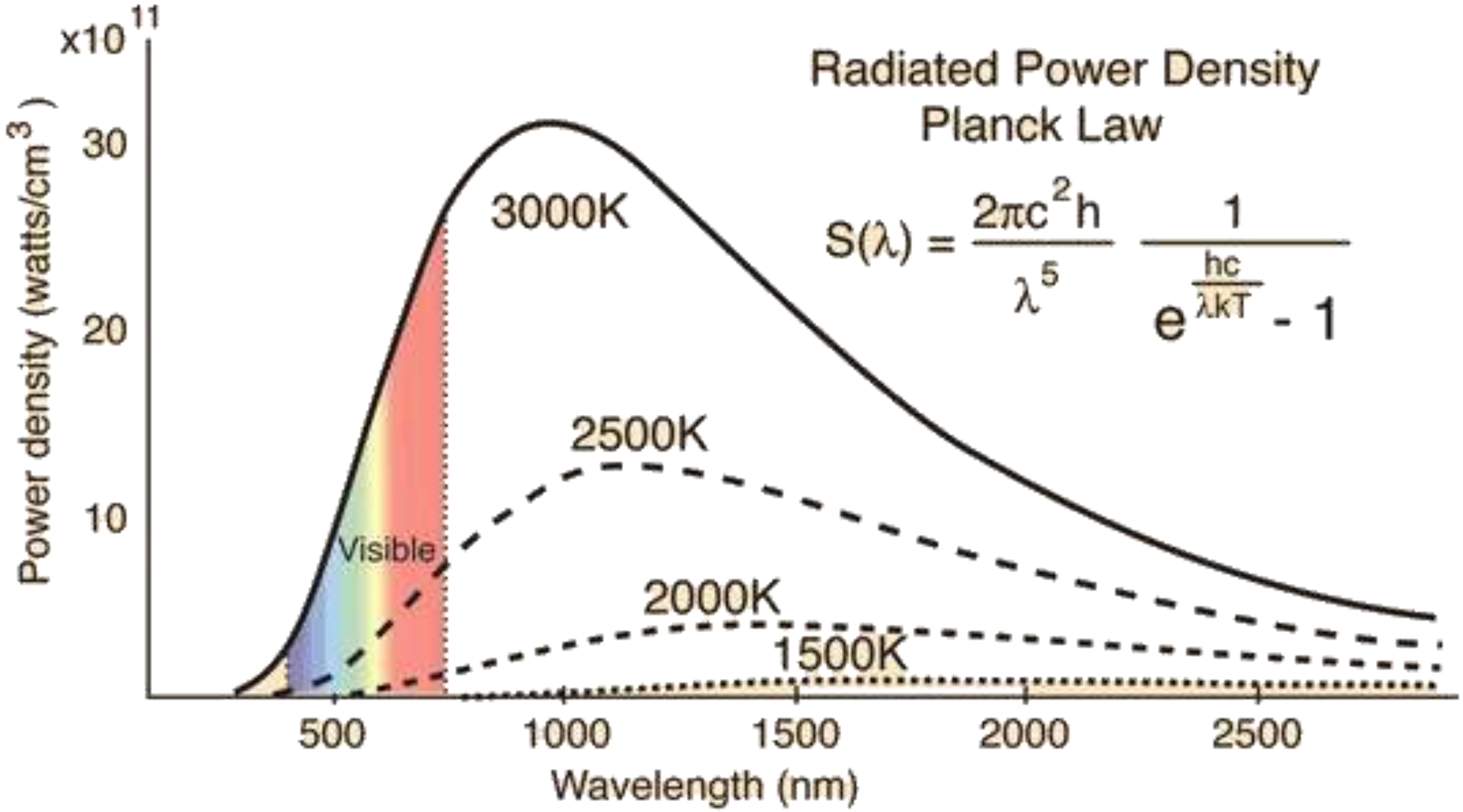

Radiated Power Density
Planck Law
$S(\lambda) = \frac{2\pi c^2 h}{\lambda^5} \frac{1}{e^{\frac{hc}{\lambda kT}} - 1}$
x10^11
Power density (watts/cm^3)
30
20
10
3000K
2500K
2000K
1500K
Visible
500
1000
1500
2000
2500
Wavelength (nm)

The photospheric spectrum

- $$I_\lambda(\tau_\lambda) = I_\lambda(0)e^{-\tau_\lambda} + \int_0^{\tau_\lambda} S_\lambda(\tau)\, e^{(t_\lambda - \tau_\lambda)}\, dt_\lambda$$

- To solve the RT equation we need $S_\lambda(\tau)$, $I_\lambda(0)$
- Photosphere assumed in LTE ($S_\lambda = B_\lambda(T)$)
- LTE – The mean free path is very small compared to the scale T changes
- LTE can be described by a single T for the distribution of energy in a small volume
- In LTE the radiation field can be described by the equations of TE characterized by the local T ($S_\lambda = B_\lambda(T)$)

The photospheric spectrum

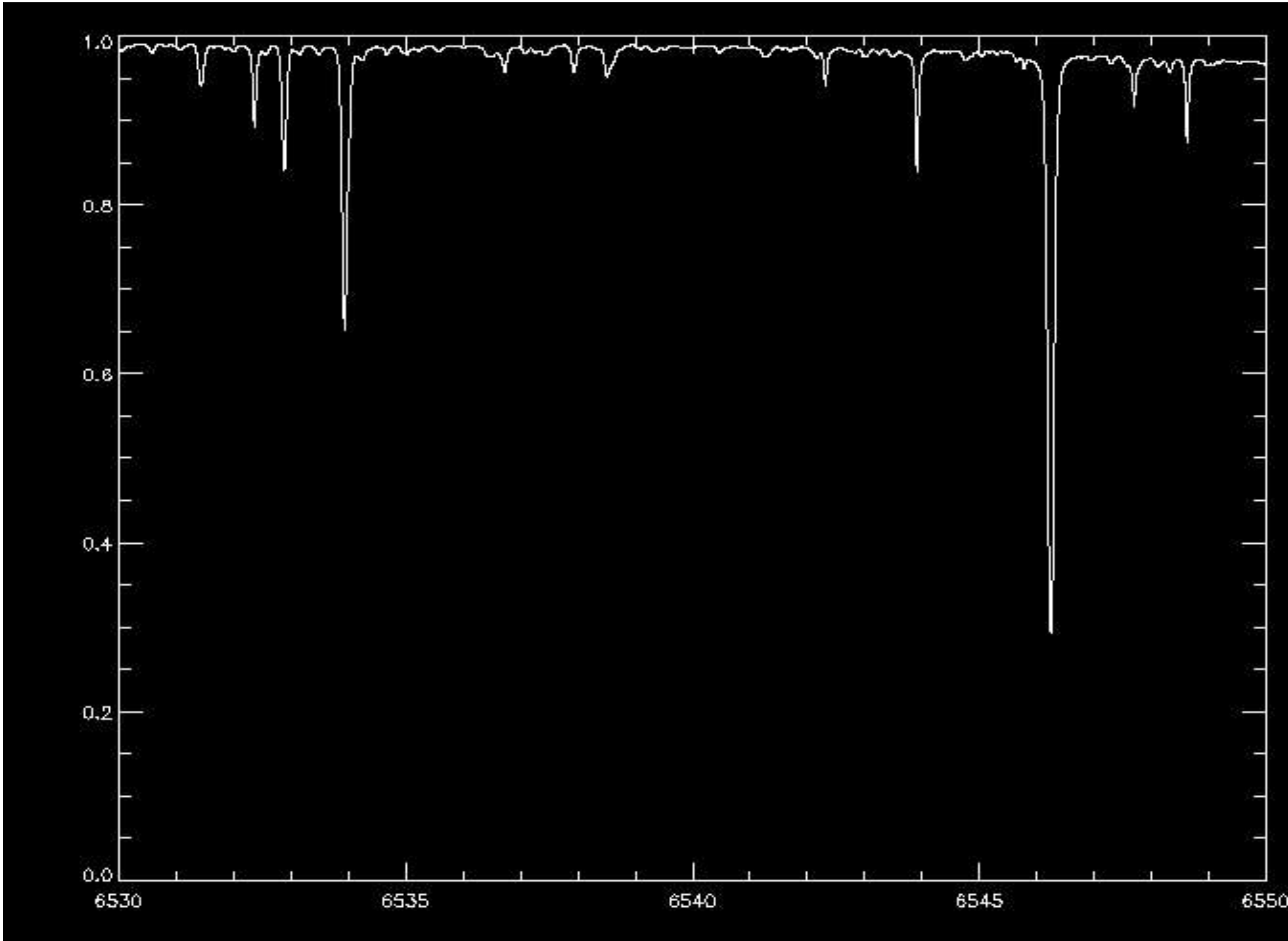

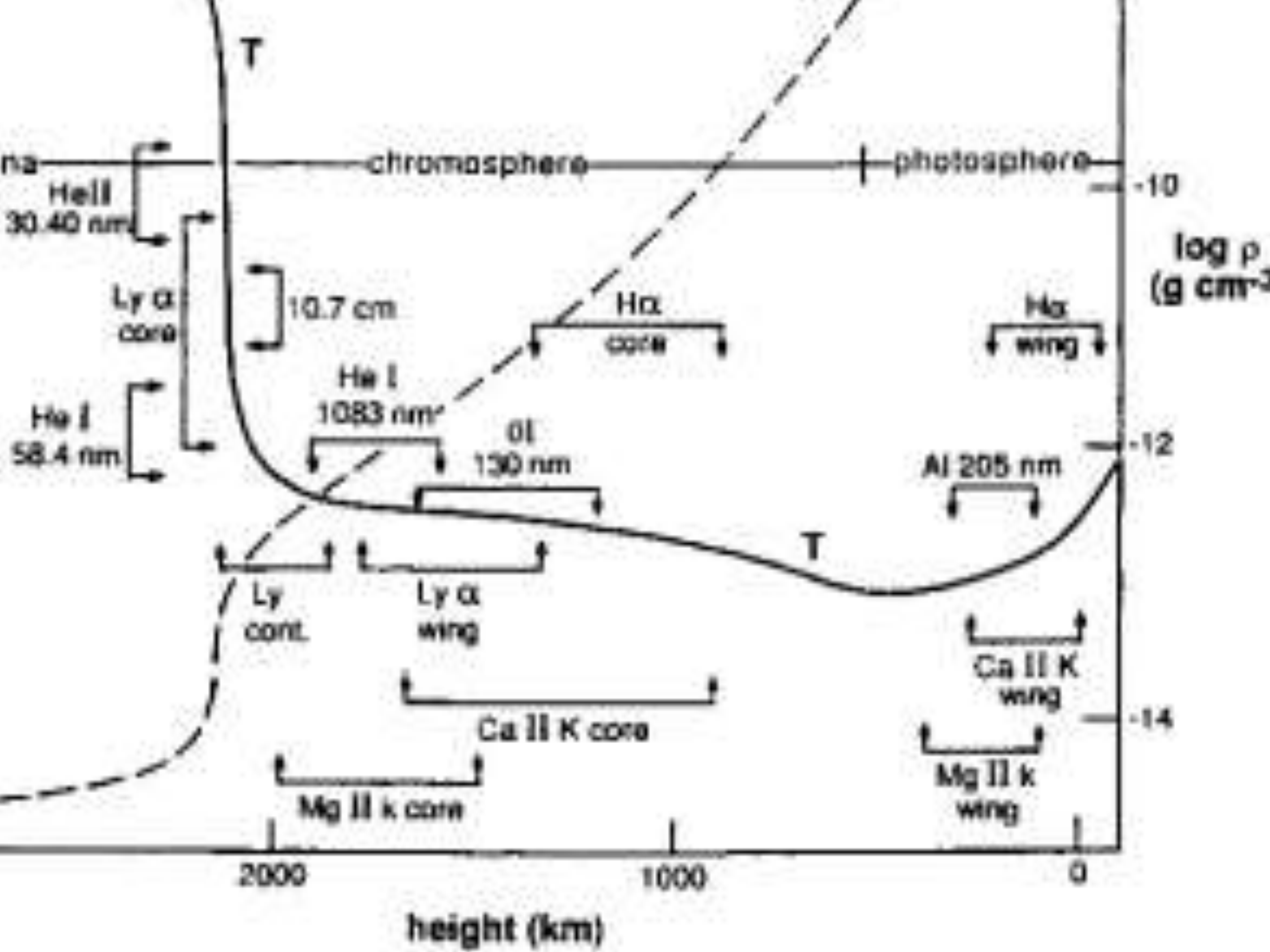

T
na
chromosphere
photosphere
He II
30.40 nm
Ly α
core
10.7 cm
Hα
core
Hα
wing
He I
1083 nm
He I
58.4 nm
OI
130 nm
Al 205 nm
-10
-12
-14
log ρ
(g cm
T
Ly
cont.
Ly α
wing
Ca II K
wing
Ca II K core
Mg II k core
Mg II k
wing
2000
1000
0
height (km)

S_λ Emission vs absorption lines

- S_λ - Source function (emission / absorption)
- Photosphere

T decreasing with height

S_λ decreasing with height leads to the formation of absorption lines in the photosphere

- Emission lines - S_λ must increase with height

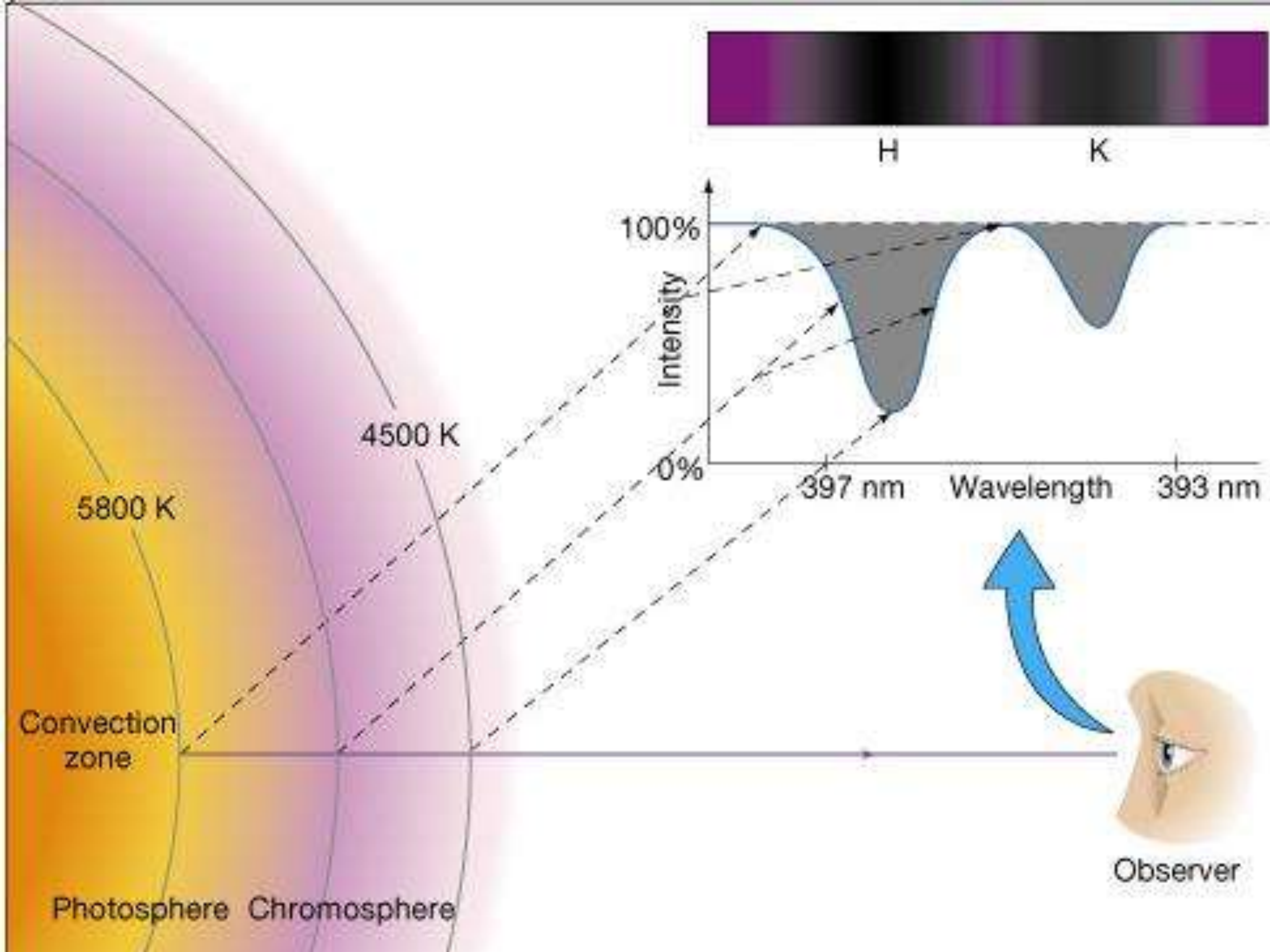
H
K
100%
Intensity
0%
397 nm
Wavelength
393 nm
4500 K
5800 K
Convection zone
Observer
Photosphere
Chromosphere

The photospheric spectrum

- Different parts of the line profile are formed at different heights in the lower atmosphere
- T and therefore S_λ decreases with height
- In the upper photosphere/temperature minimum S is lower than in the deeper layers
- Direct mapping between variation in S and line profile

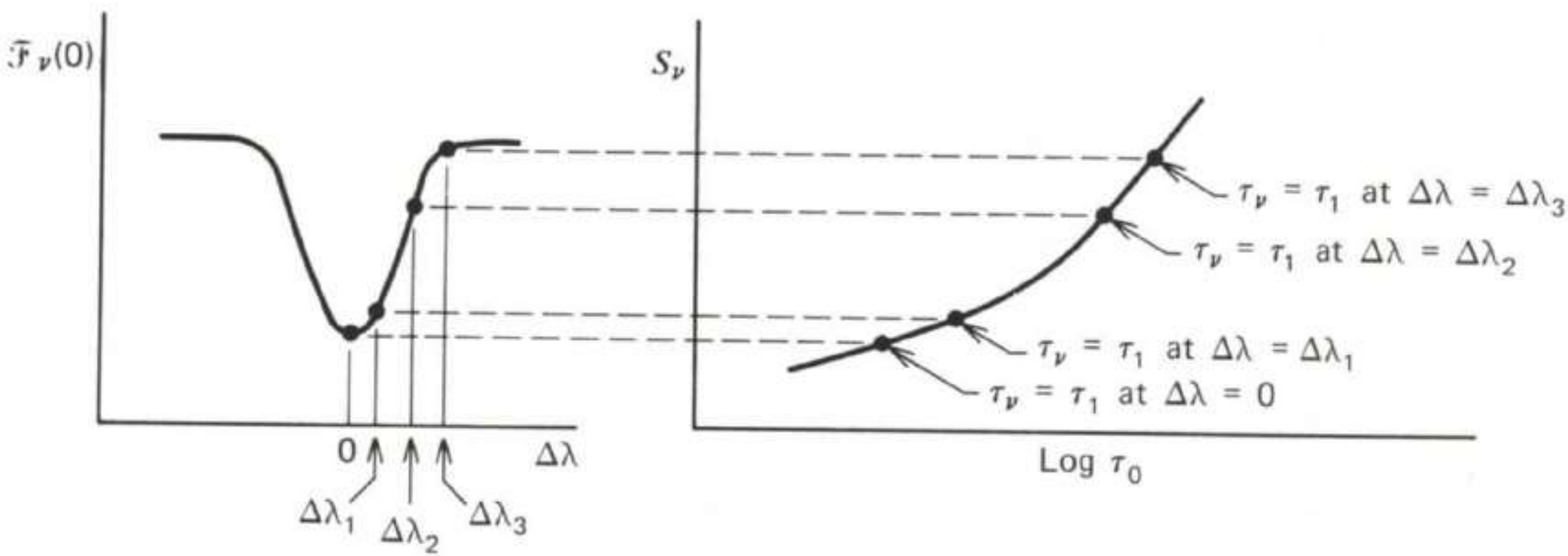

Limb darkening

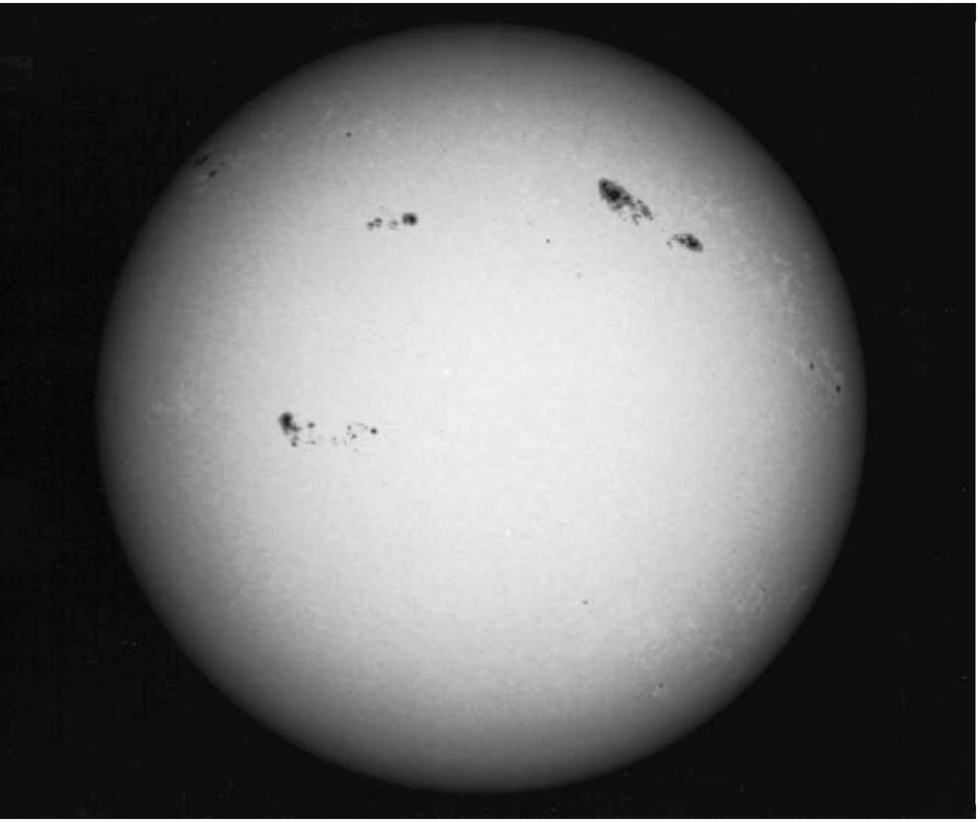

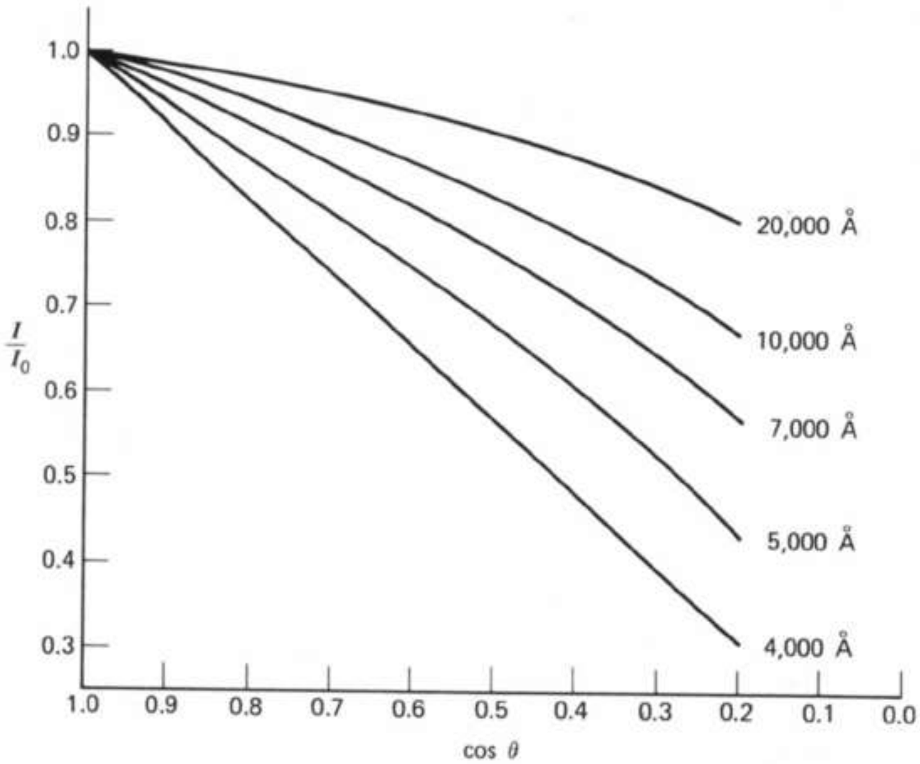

T decreases with height in the photosphere

Photosphere is in LTE hence $S_\lambda = B(T)$

Source Function S_λ decreases with height (follows B(T))

At the limb we look higher in the atmosphere (for a given λ) where the photospheric T is lower hence less intensity than disk center

VAL Model

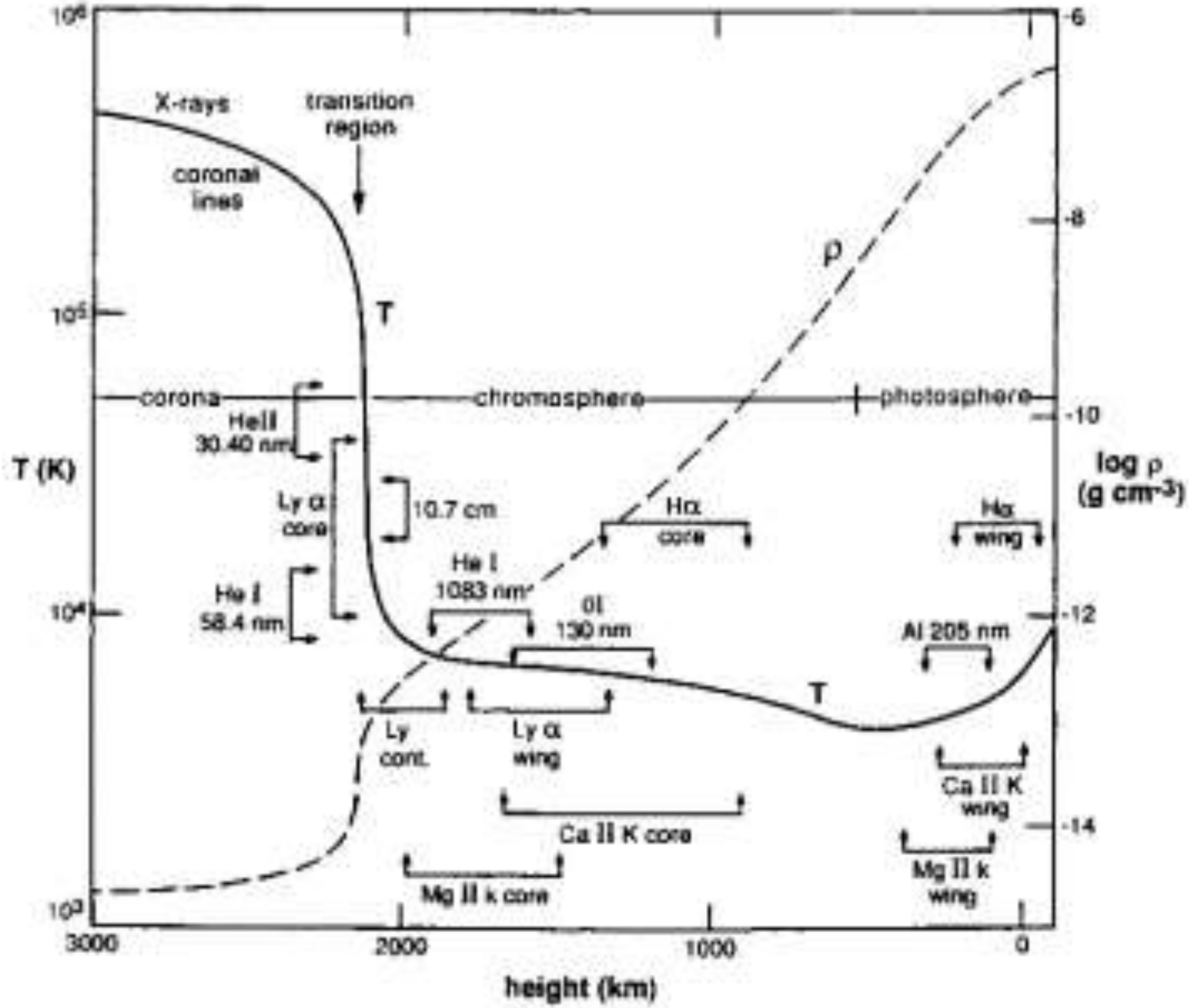

Vernazza et al. (1976, 1981)

Chromosphere - Colour Sphere

- Temperature: 20,000 K or more
- Density: 30,000 times less dense than air
- $\beta < 1$

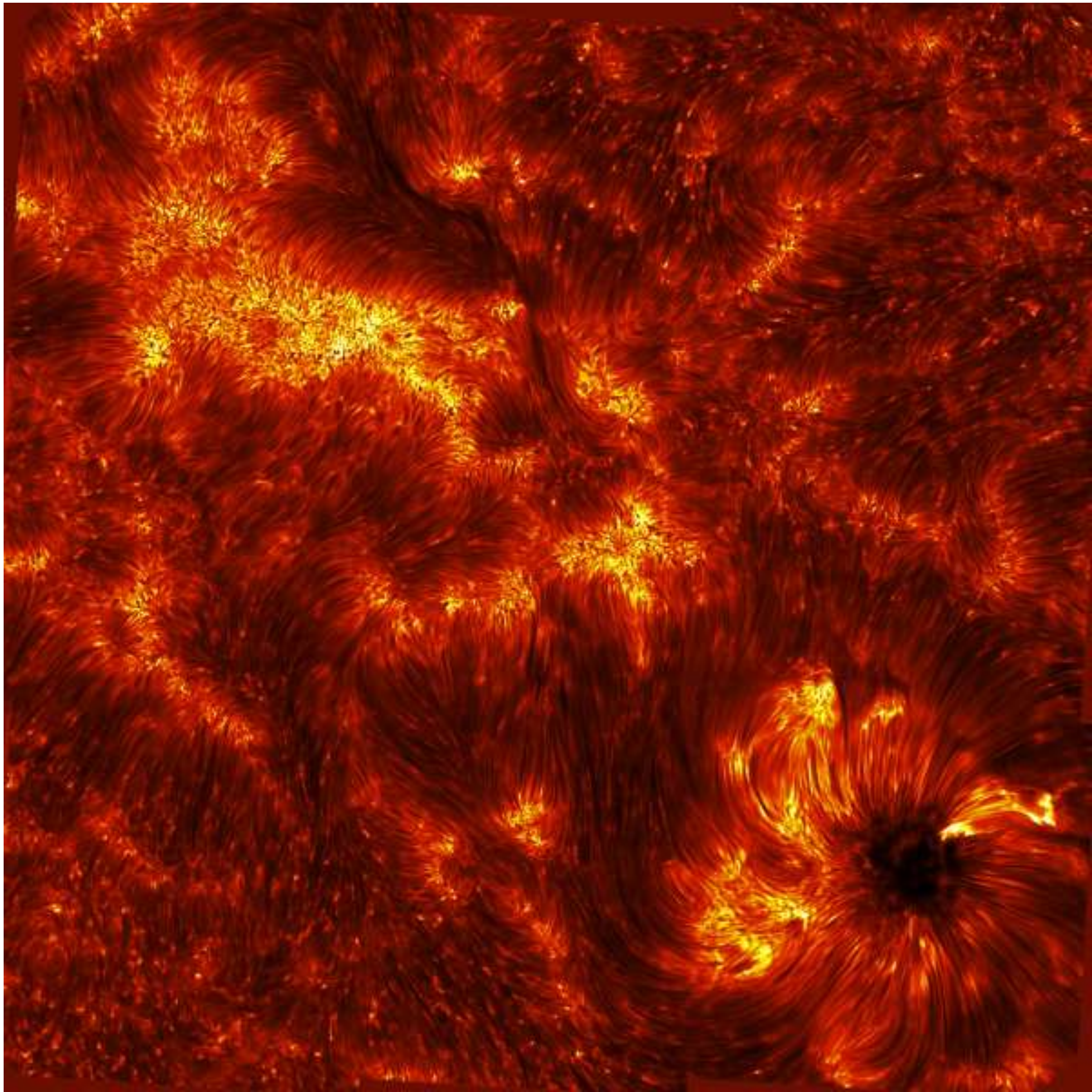

The magnetic canopy
Layer of magnetic field parallel to the solar surface

- Magnetic pressure at the flux tube surface $B^2/2\mu = p_{ext} - p_{int}$
- P_{ext} decreases exponential with height
- Flux tube forced horizontally and expands

- The magnetic field can not be confined by the gas pressure and spreads out

- Canopy Located in the low chromosphere overlying the "'field – free" photosphere

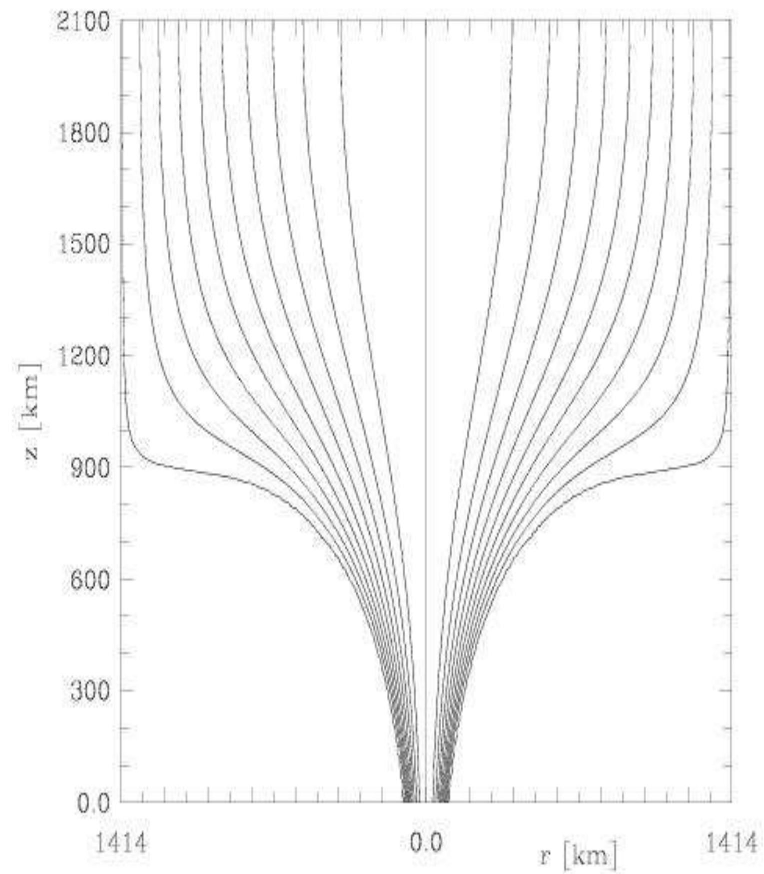

Gabriel 1976, Dowdy 1986, Steiner 2005


©mongabay.com

Absorption lines with emission cores

- In the chromosphere the T increases with height
- S_λ increasing with height - Emission lines in the chromosphere

Emission cores: Emission at greater heights dominates over absorption

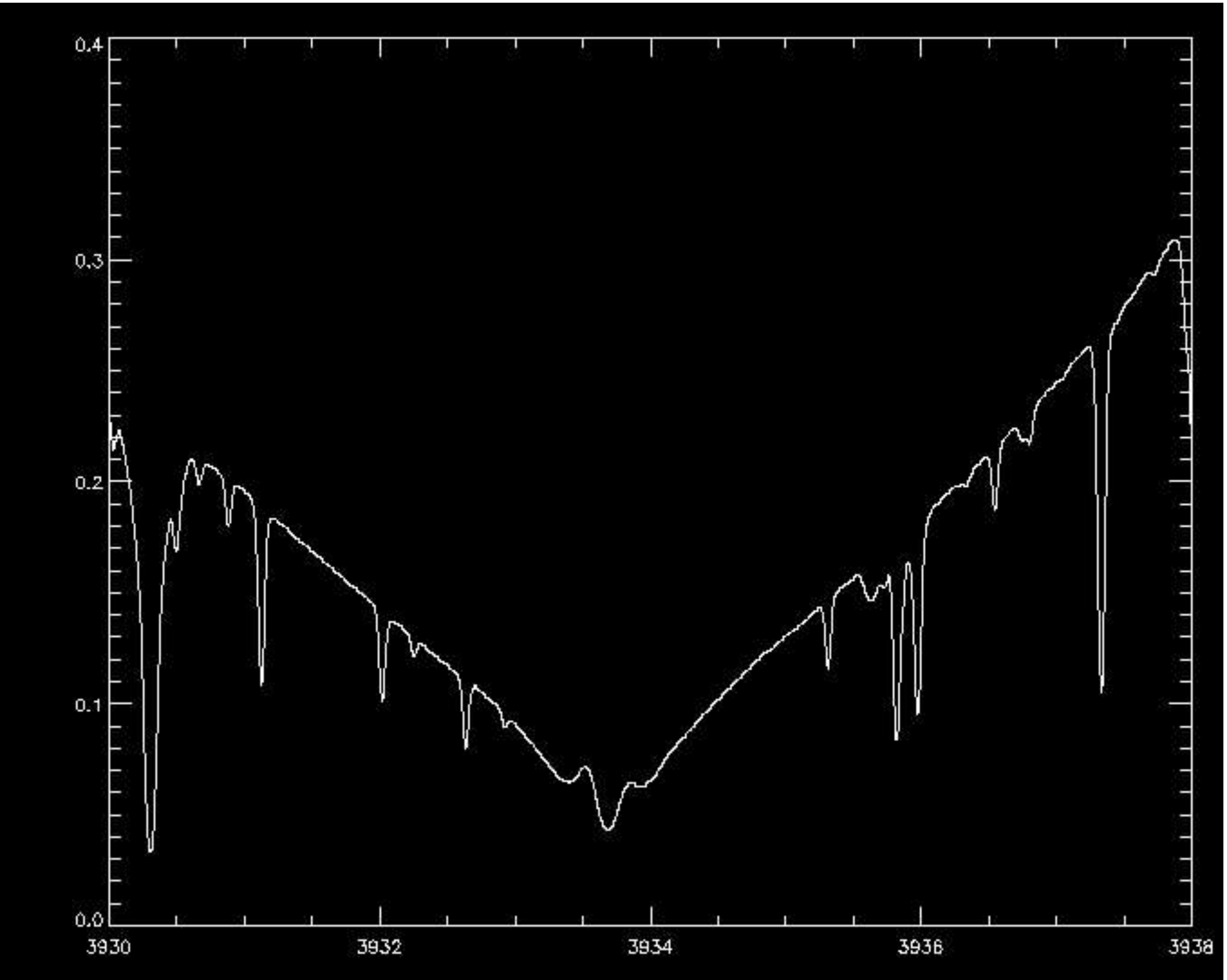

Emission cores in the Ca II H&K lines

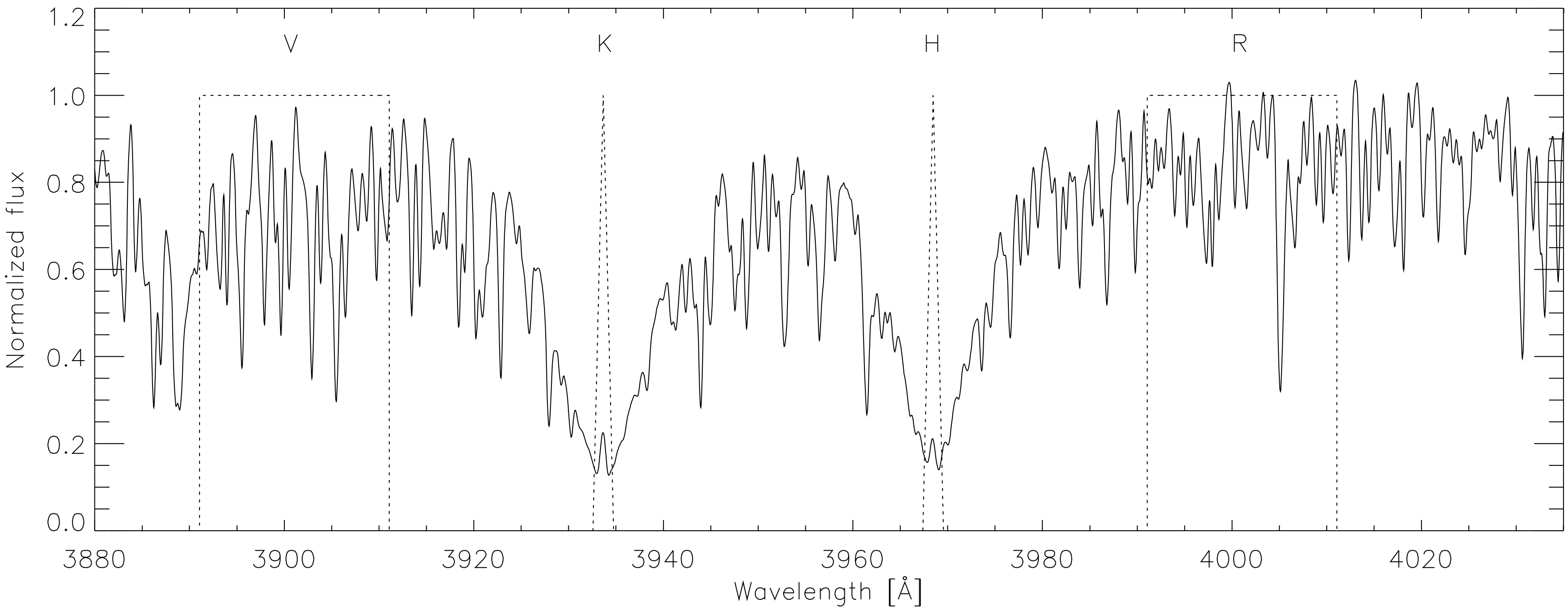

Vaughan et al. 1978

Contribution Functions

- Different layers contribute to the intensity of a given wavelength/frequency
- The intensity from different layers is described with the contribution function

$$I_\nu = \int_{z_0}^{z} C_i \, dz = \int_{z_0}^{z} S_\nu \tau_\nu e^{-\tau_\nu} \frac{\chi_\nu}{\tau_\nu} dz$$

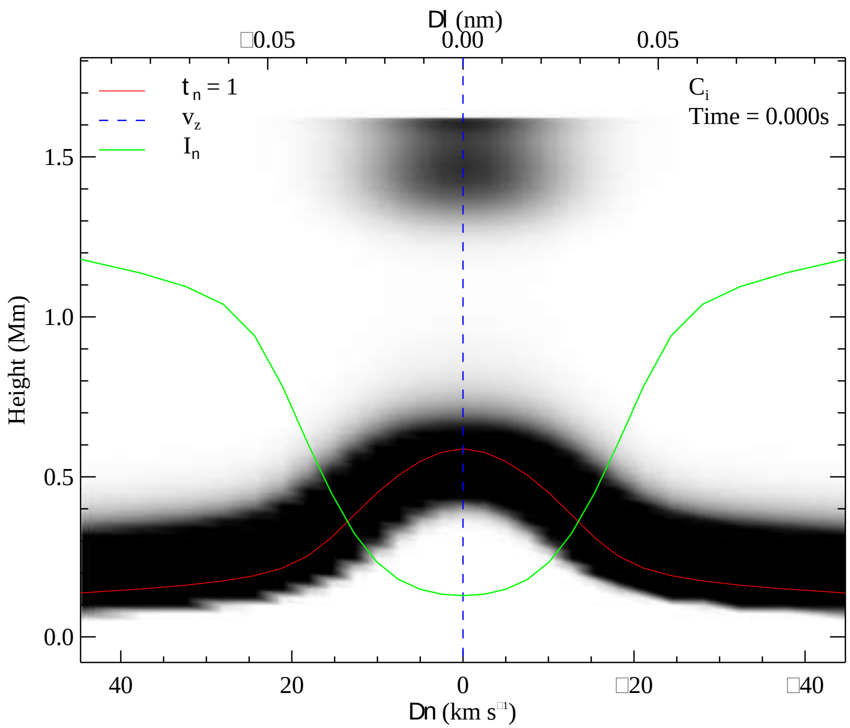

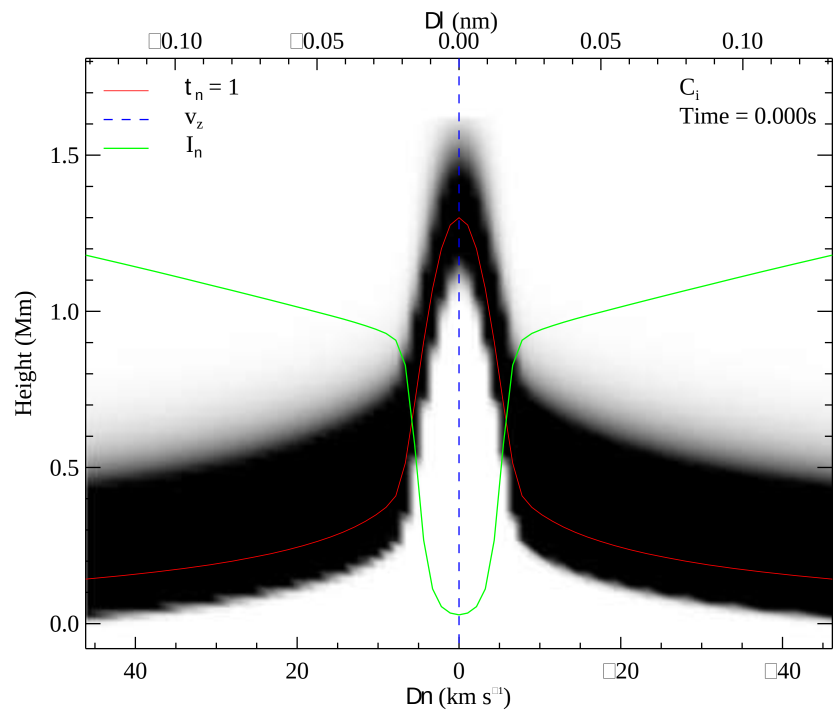

- **Green** - Line profile
- **The darker the scale** the more the emission

Hα - The Dynamic Chromosphere

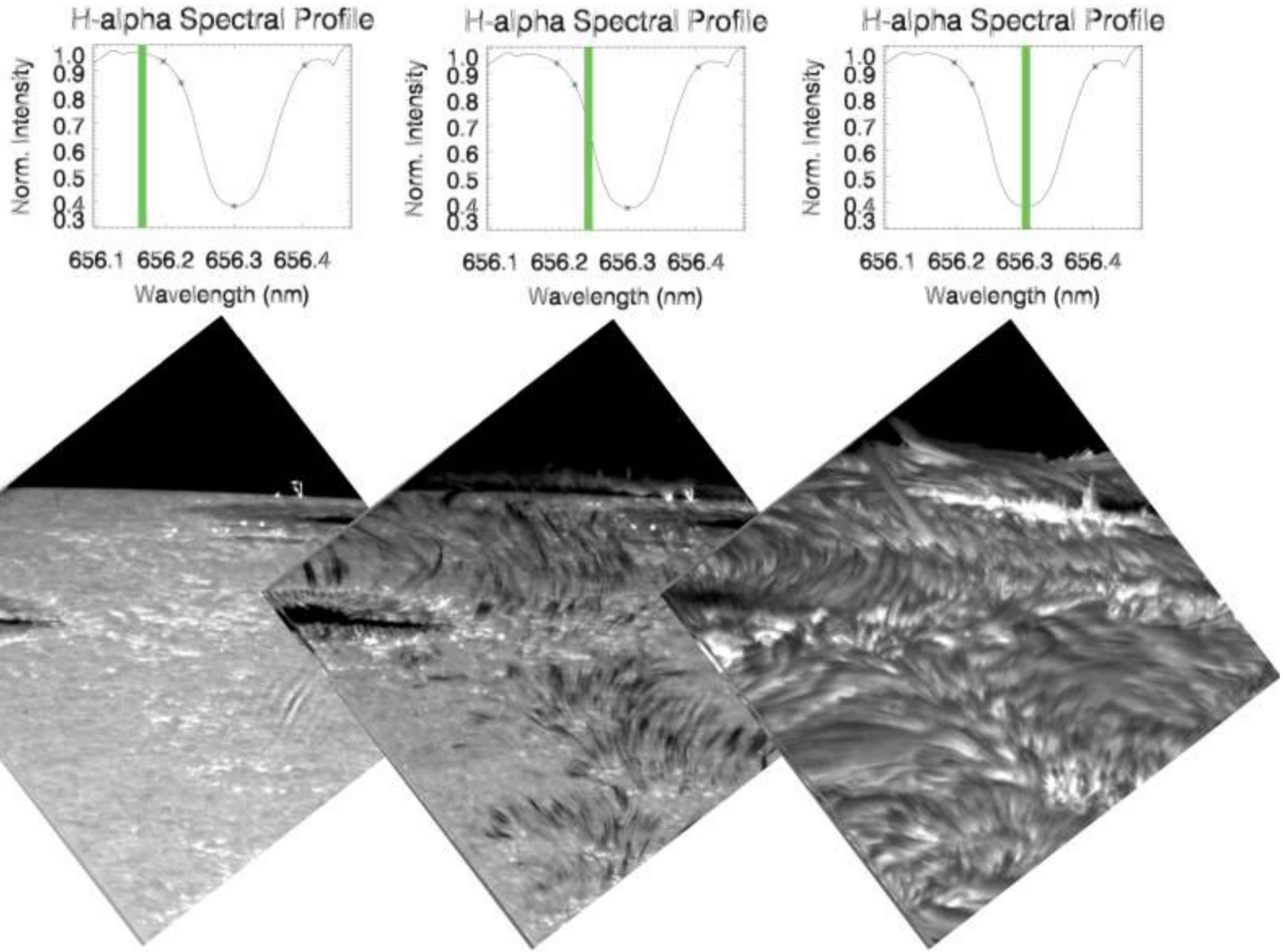

Credit: E. Scullion, Northumbria

Model atmospheres

- $I_\lambda(\tau_\lambda) = I_\lambda(0)e^{-\tau_\lambda} + \int_0^{\tau_\lambda} S_\lambda \, e^{(t_\lambda - \tau_\lambda)} \, d\, t_\lambda$

- Start with an initial "guess" of T_{eff}, $T(\tau)$,
- Abundances, opacity/absorption coefficient
- Use n_e to calculate opacity at any given P ,T and recalculate n_e until convergence is achieved
- When convergence is achieved we have $P(\tau)$, and $n_e(\tau)$, $T(\tau)$

Model atmospheres

- Solve simultaneously
  - Statistical equilibrium (transitions up = transitions down)
  - Ionization equilibrium (ionizations = recombinations)
  - Radiative transfer equations
- Calculations might consider ions with 30 levels or more
- Hundreds of separate transitions between individual levels
- For each point in the atmospheric grid the equations have to be solved simultaneously

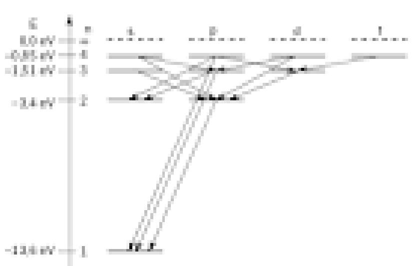

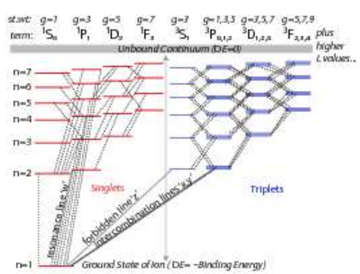

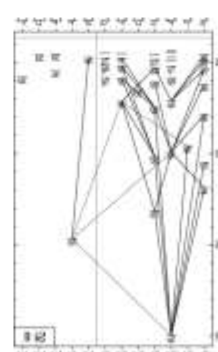

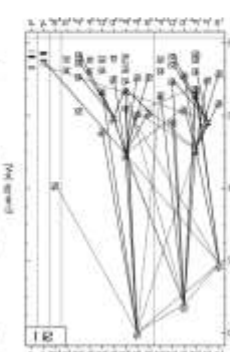

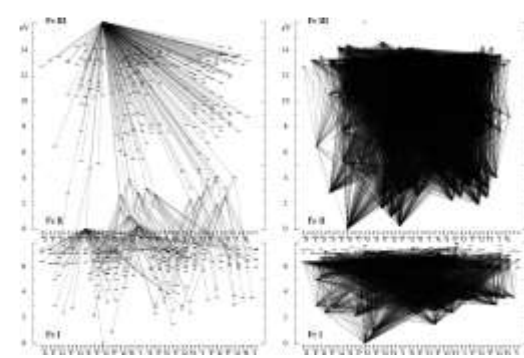

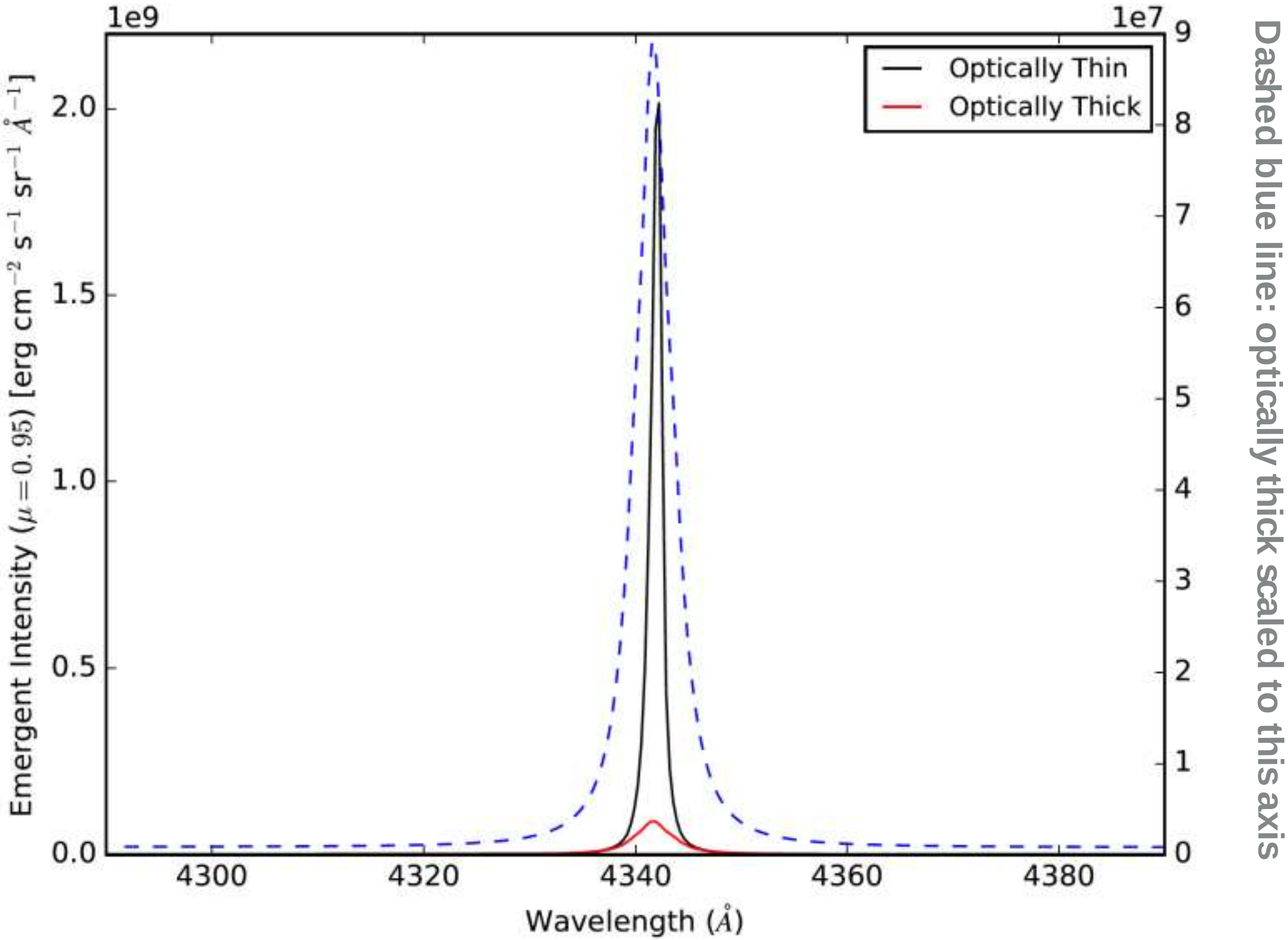

- In the optically thick case most of the original radiation (black) is attenuated (red) due to the exponential absorption term

$$I_\lambda(\tau_\lambda) = I_\lambda(0)\mathbf{e}^{-\tau_\lambda} + \int_0^{\tau_\lambda} S_\lambda\, e^{(t_\lambda - \tau_\lambda)}\, dt_\lambda$$

Credit: Kowalski

Transition region

- Thin layer that separates the chromosphere from the corona
- Radiation is not an efficient energy loss mechanism (H, He ionized)
- Conduction has to carry the energy away
- Very steep temperature gradient

  $2 \times 10^4 - 5 \times 10^5$ K in less than 100 Km
- Collisional excitation dominates; radiative excitations are rare
- Optically thin conditions

$$E_{rad} \propto n_e^2$$

$$E_{cond} \propto dT/dh$$

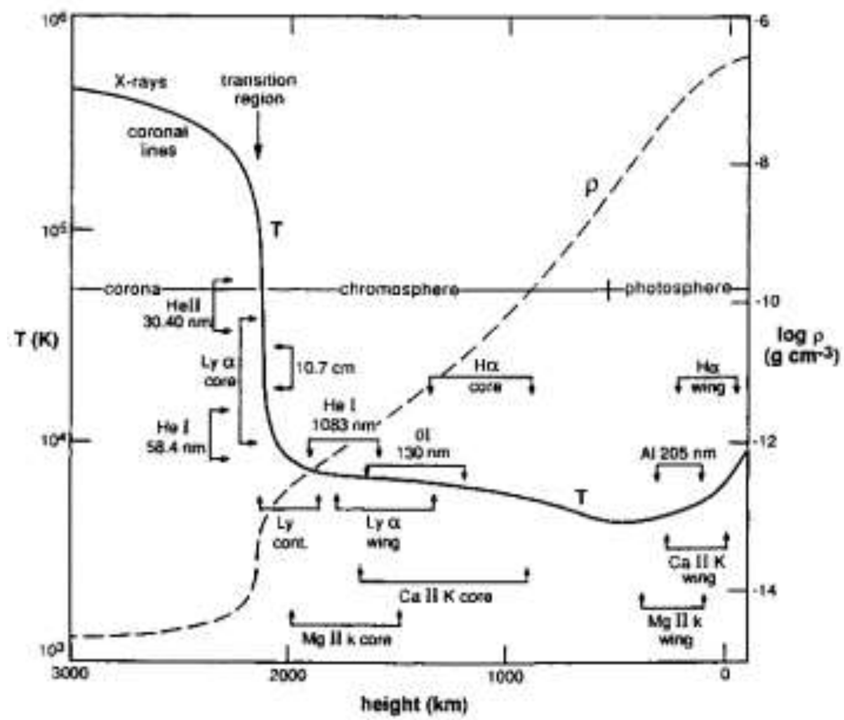

Statistical Equilibrium

Transitions up

- Radiative Excitation – $N_{12} = n_1 B_{12} J_{12}$
- Collisional Excitation – $N'_{12} = n_{12} n_e C_{12}$

Transitions down

- Radiative de-Excitation – $N_{21} = n_2 A_{21}$ (spontaneous emission)
- Collisional de-Excitation – $N_{21}' = n_2 n_e C_{21}$

In Equilibrium: $\cancel{n_1 B_{12}} J_{12} + n_{12} n_e C_{12} = n_2 A_{21} + n_2 n_e C_{21}$

Radiation field (J) in the corona is very low

Allowed transition: $n_{12} n_e C_{12} = n_2 A_{21}$

- Loops – The building blocks of the corona
- T - 1 million K (quiet) - 10 million K (very active)
- Density 300 million times less dense than air
- Collisional excitation dominates - Radiative excitations are rare
- Plasma $\beta << 1$; Magnetic pressure dominates
- Optically thin conditions

Corona

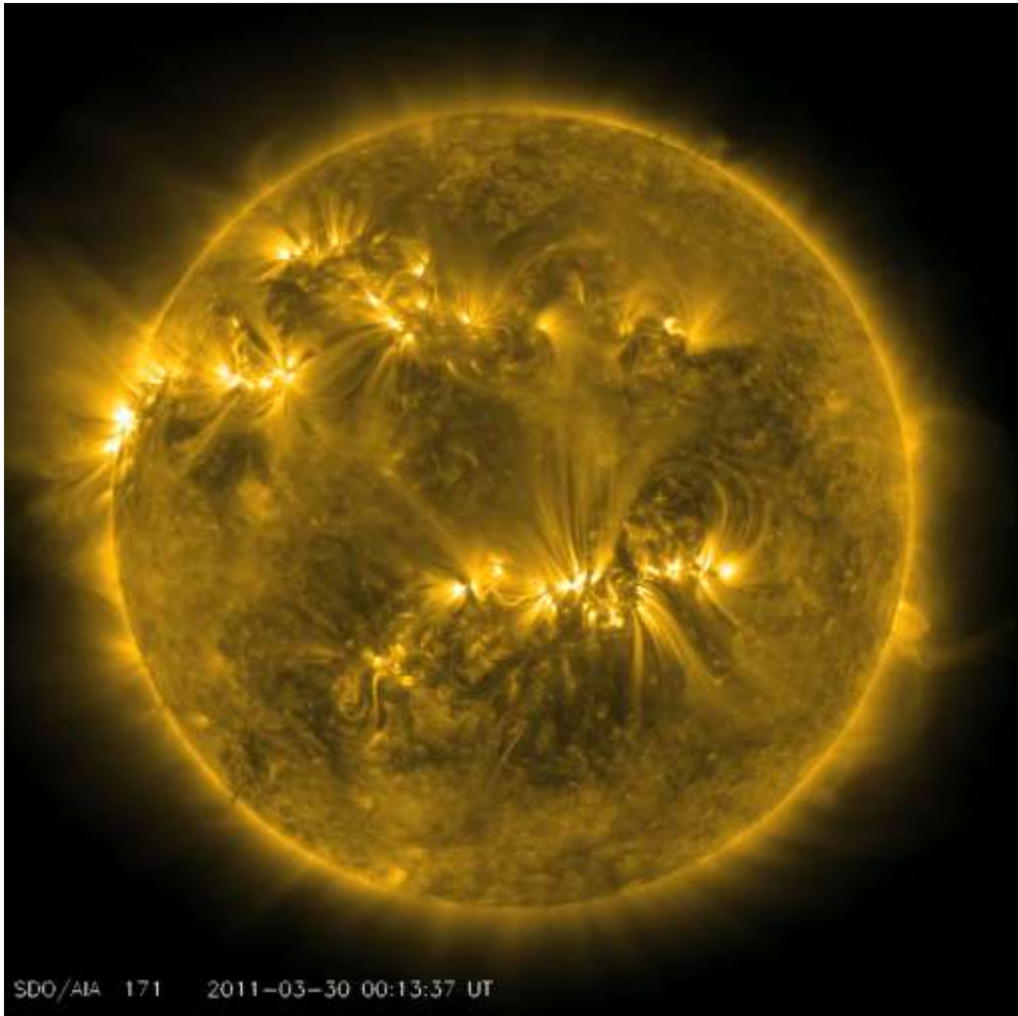

Spectrum of the TR

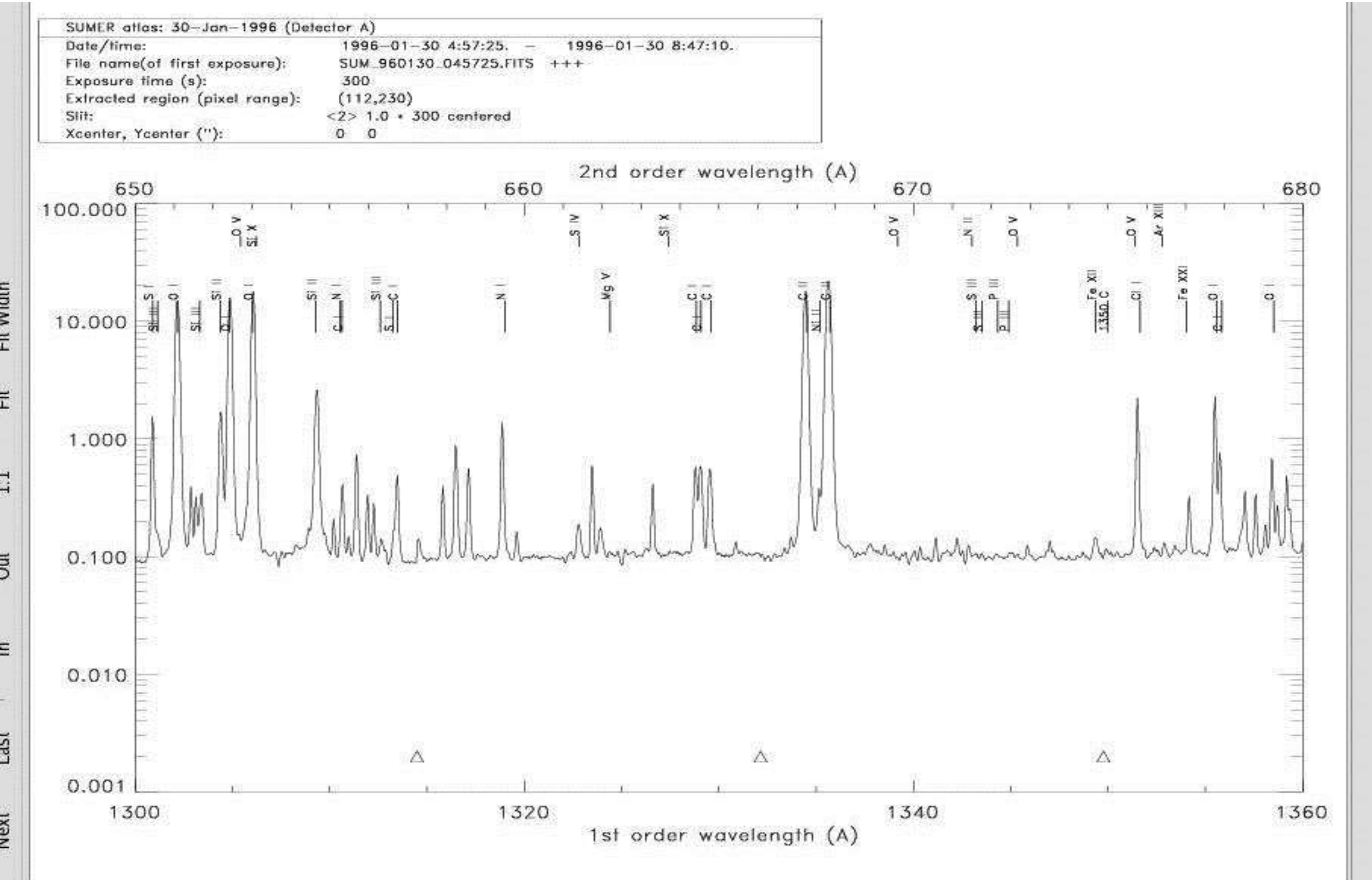

Spectrum of the Corona

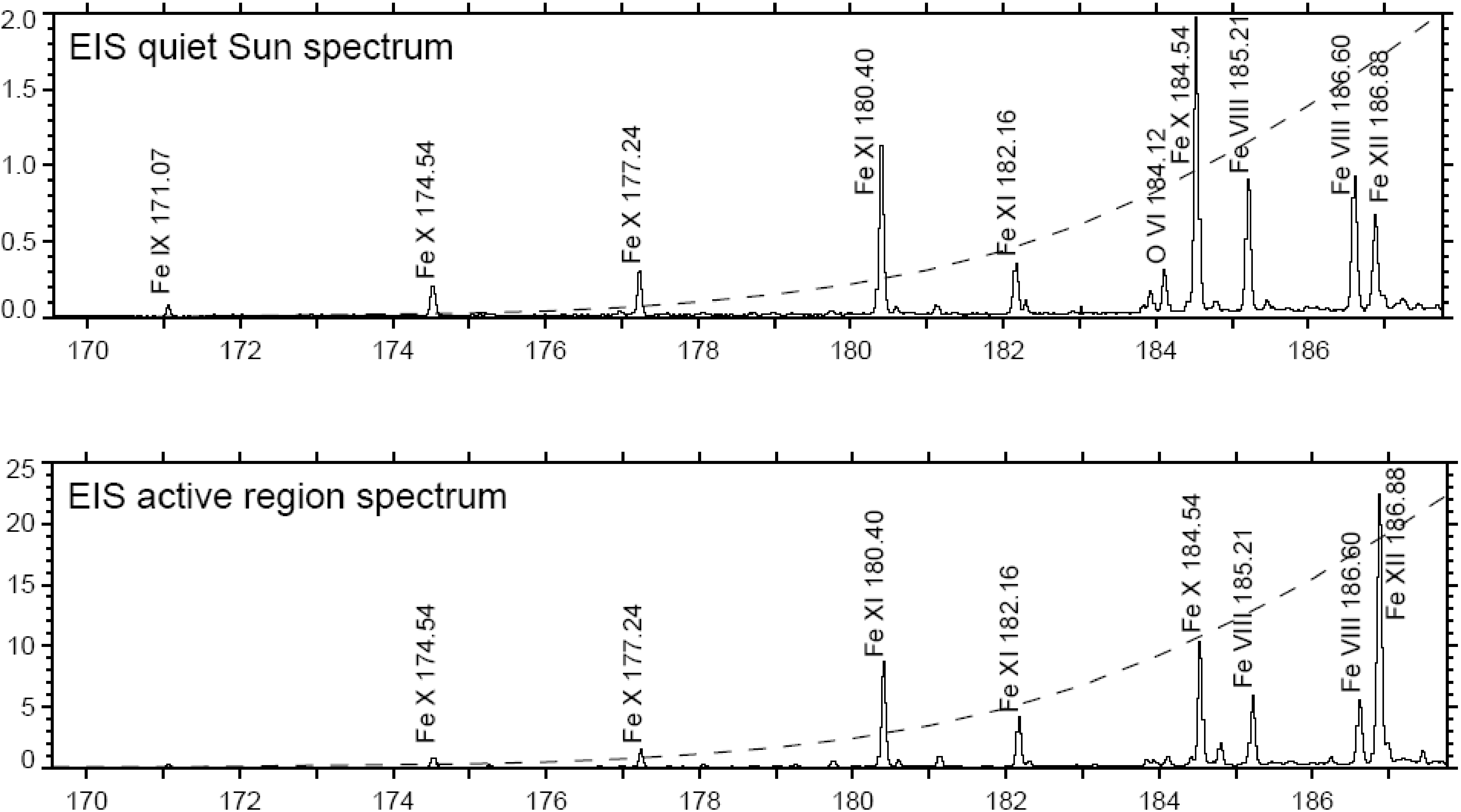

Young et al. 2007

What parameters determine the flux of an optically thin emission line?

The flux of an optically thin line

$$F_{21} = \frac{8.63 \times 10^{-6} h\nu_{21} 0.8\, A_{el} \Omega_{12}}{4\pi r^2 g_1} G(T) EM$$

$$G(T) = \frac{n_{ion}}{n_{el}} T^{-1/2} e^{\frac{-h\nu_{21}}{kT}}$$

$$EM = \int_{\Delta V} n_e^2 dV$$

- Elemental abundance - A_{el}
- Atomic data – Ω_{12} g_1
- Ionization balance – G (T)
- Emission measure – EM
- Distance - r

Limb Brightening

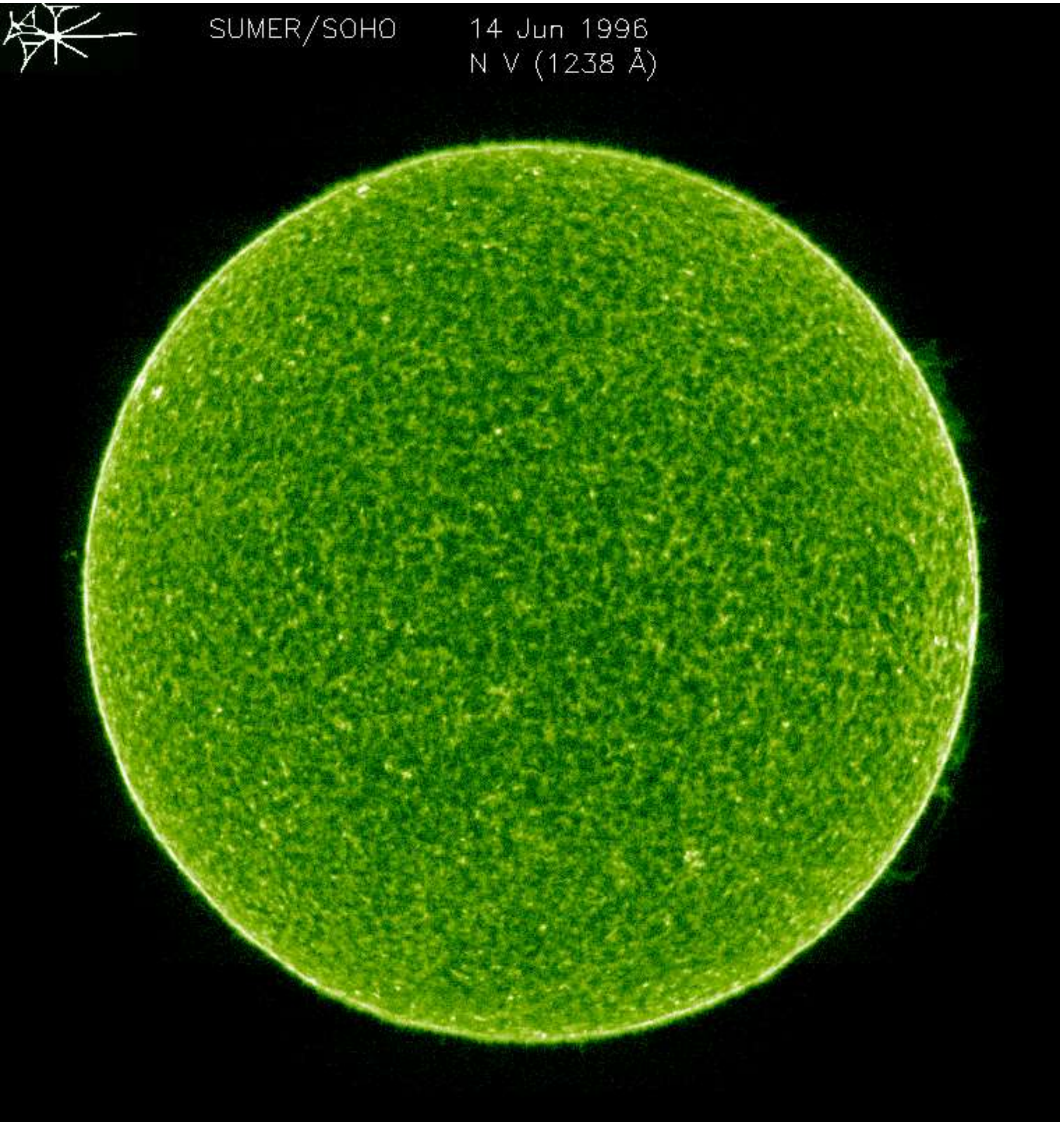

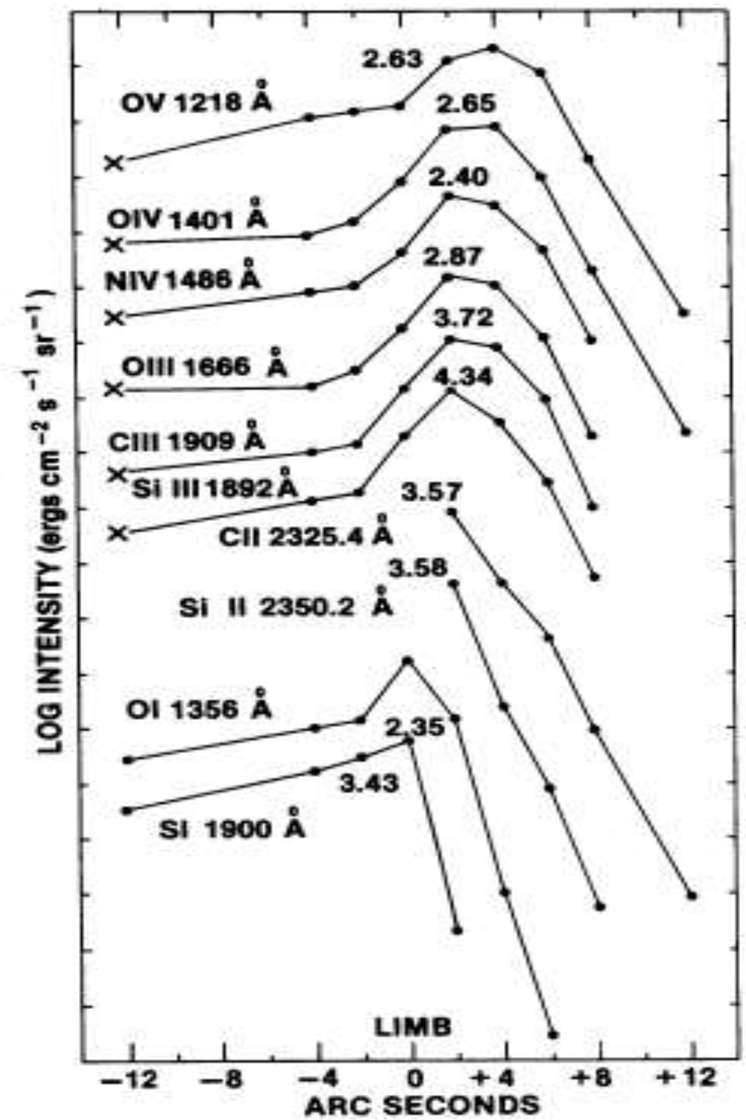

Mariska 1978

Upper chromosphere/TR : Brighter at the limb than disk center

Path length increases therefore optically thin line intensity increases

Emission Measure

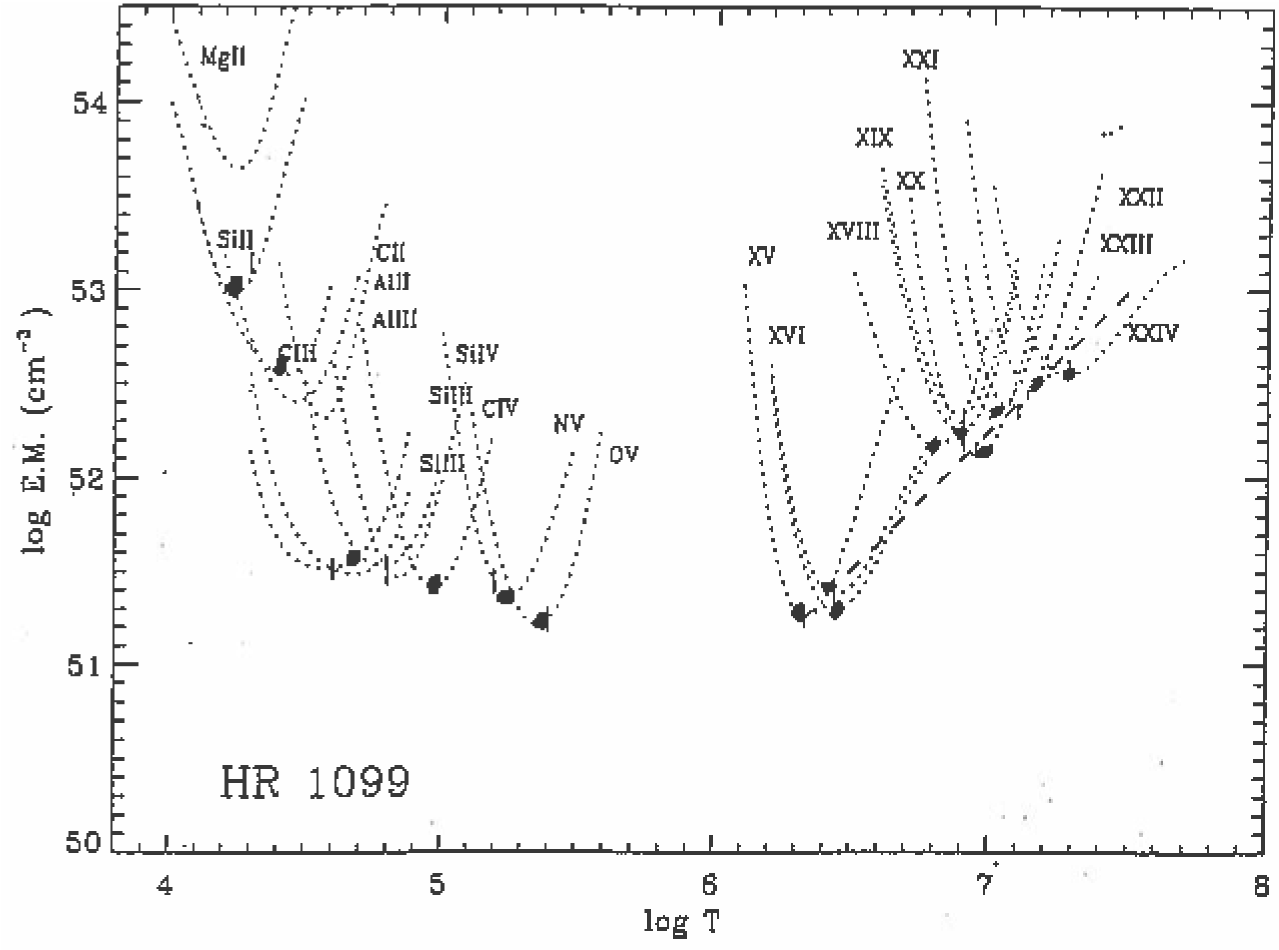

$$EM = \int_{\Delta V} n_e^2 dV$$

Amount of material at a given temperature

Emission Measure Distributions

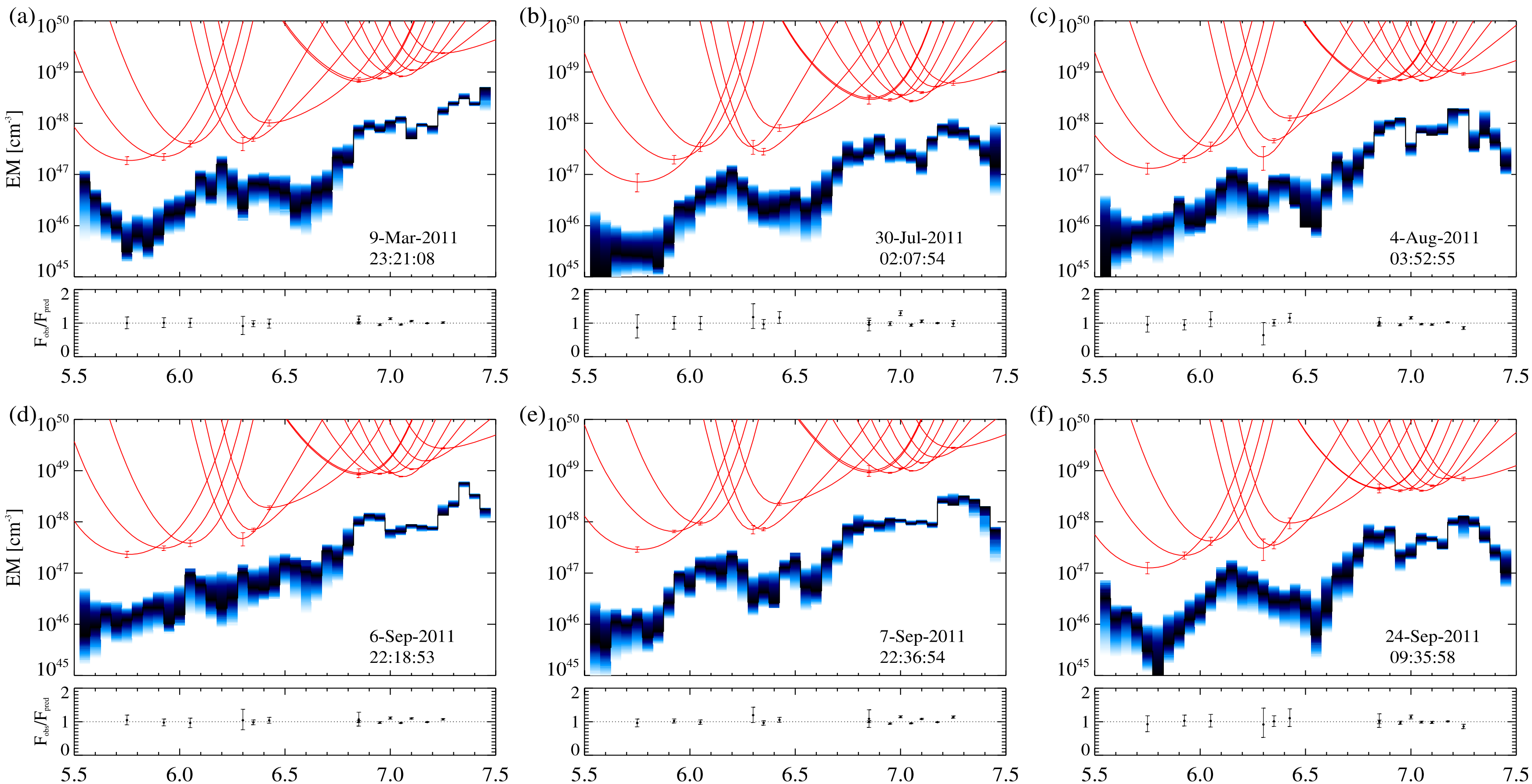

Kennedy et al. 2015

Ionic Fractions

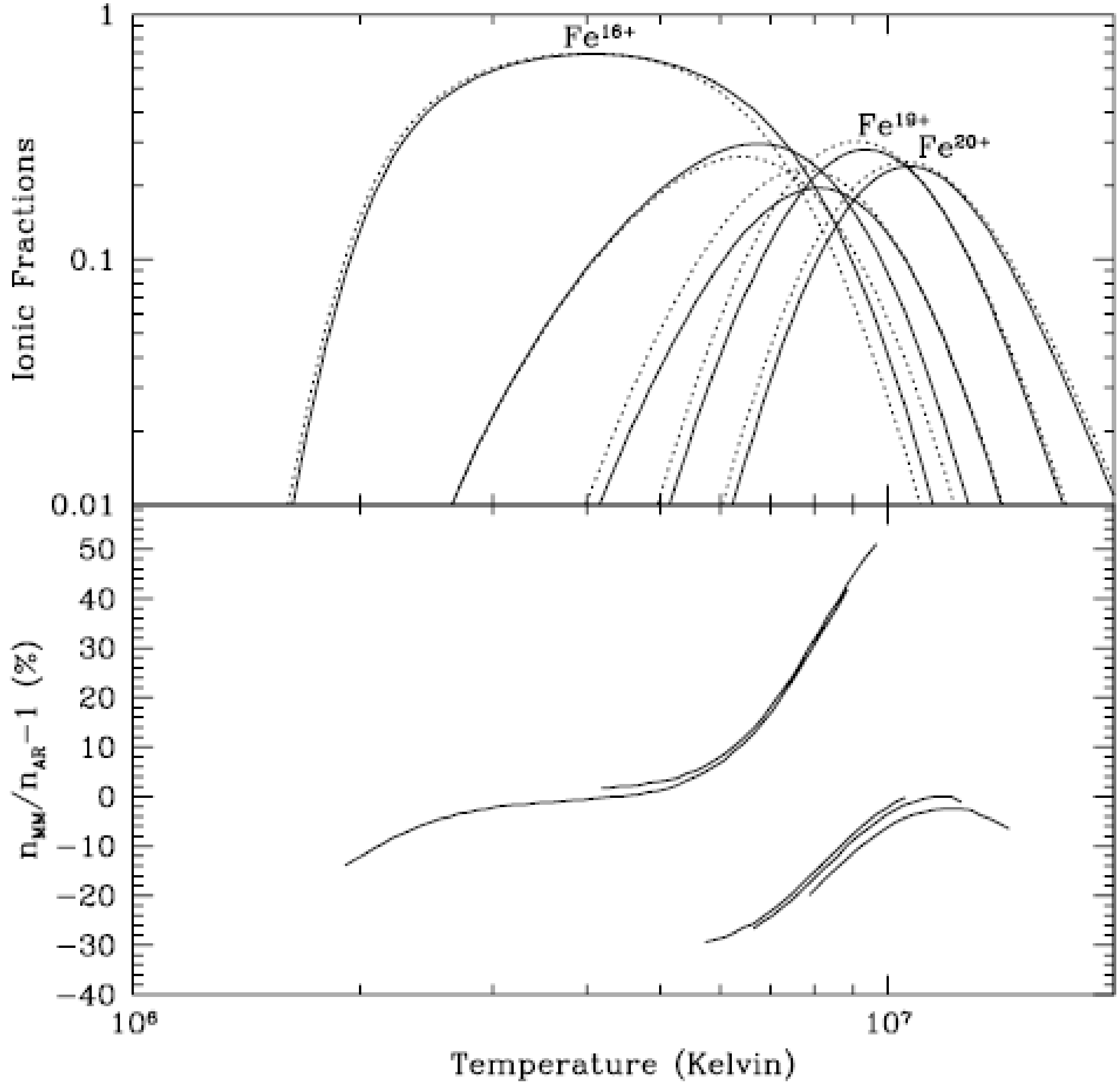

Mazzotta et al, 1998

Optically Thin Emission – Density Diagnostics

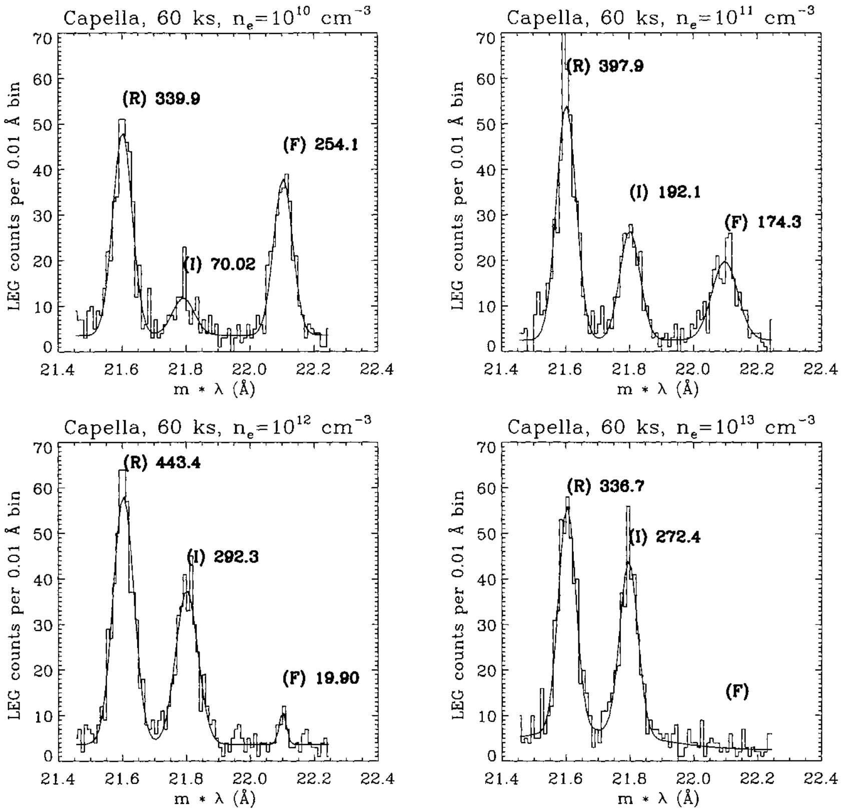

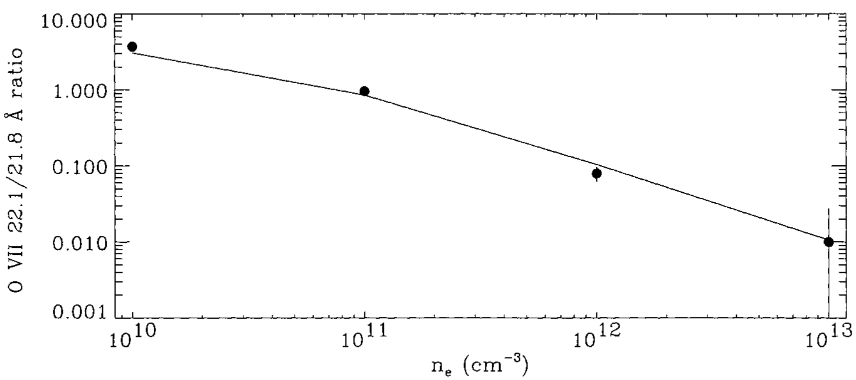

Allowed transition: $n_{12} n_e C_{12} = n_2 A_{21}$

Forbidden transition: $n_{1f} n_e C_{1f} = n_2 A_{f1} + n_f n_e C_{f1}$

$$\frac{F_{fi}}{F_{21}} \propto \frac{A_{f1}}{A_{f1} + n_e C_{f1}}$$

Electron Densities – Fe XXI

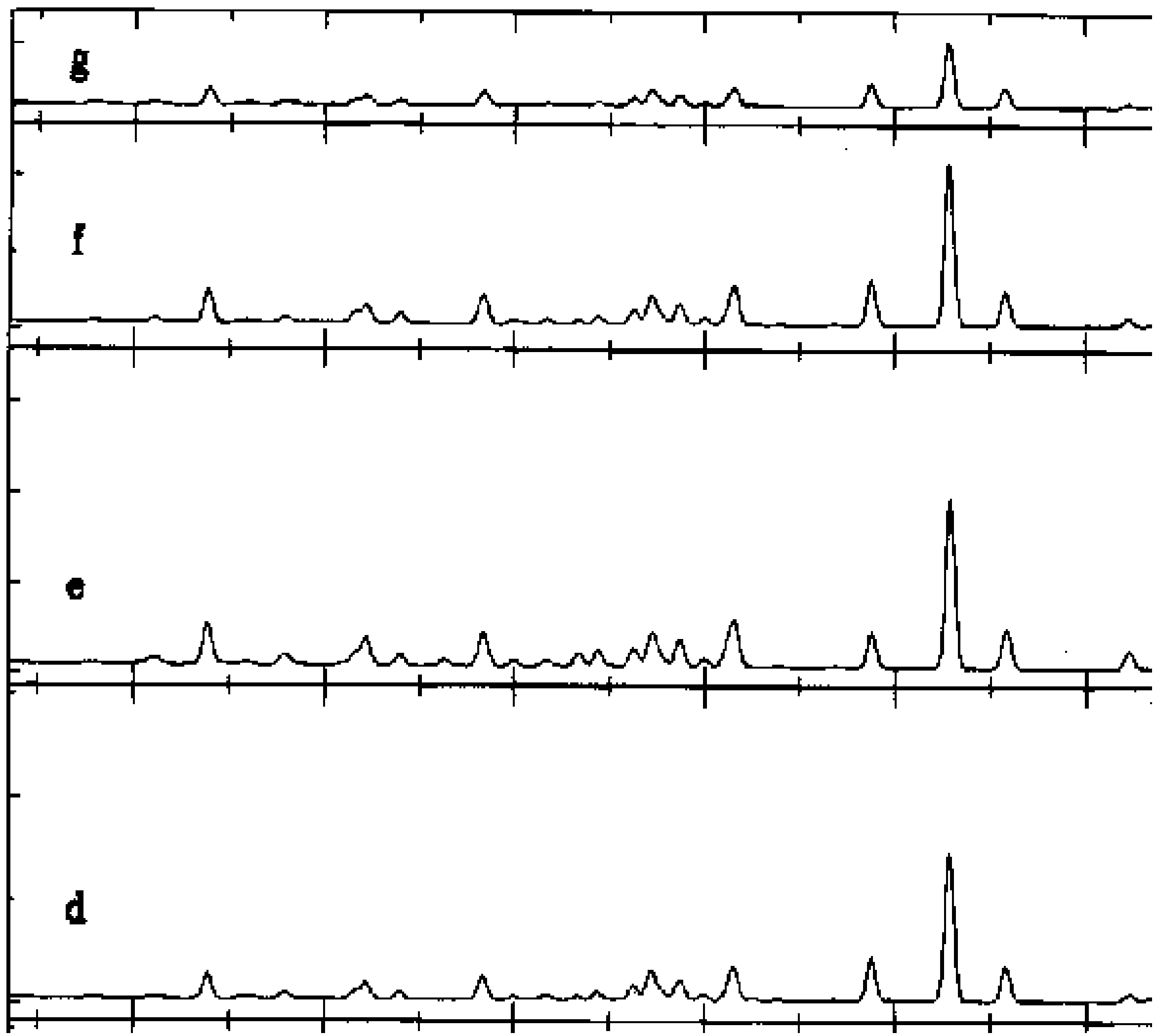

- Fe XXI line ratios (142/128)
- Electron densities in stellar flares more than 10 times higher than solar flares

Monsignori-Fossi et al. ApJ 1996

Velocities from line profiles

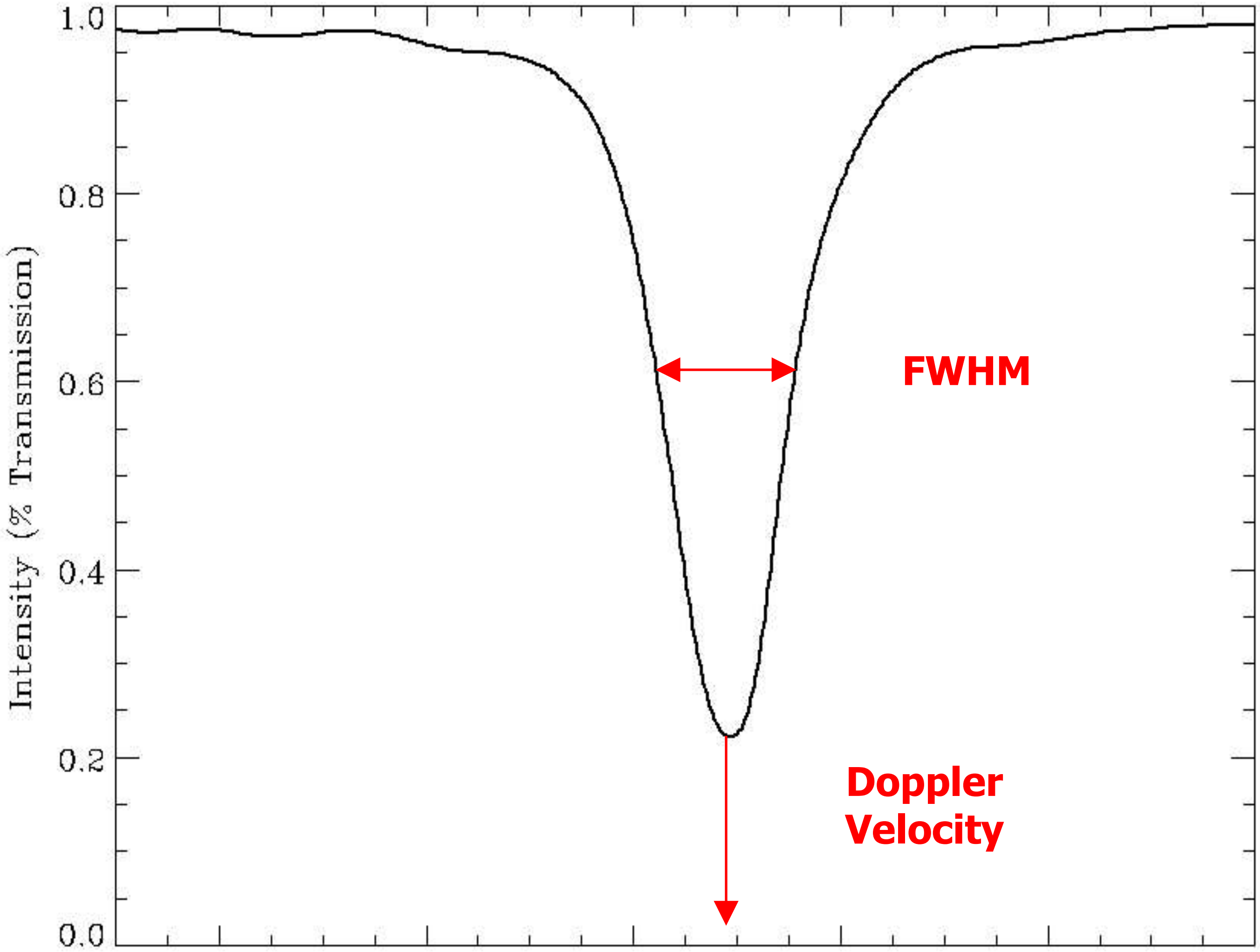

$$\frac{v_{los}}{c} = \frac{\Delta\lambda}{\lambda_0}$$

$$\Delta\lambda_{FWHM} = \frac{\lambda_0}{c}\sqrt{\frac{2kT}{m}}$$

- $\Delta\lambda_{obs}^2 = 4 \ln(2)\, \Delta\lambda^2 + \Delta\lambda_i^2$ $\Delta\lambda_i$ = instrumental width
- $\Delta\lambda^2 = (2kT/m + \xi^2)\,(\lambda/c)^2$

pre-flare post-impulsive impulsive

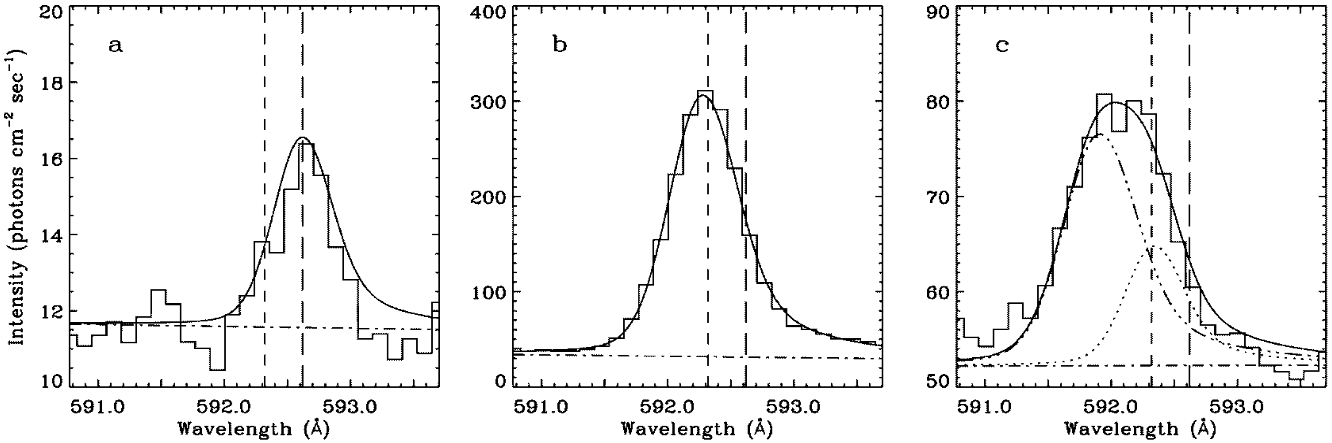

Complex line profiles can be disentangled using multiple Gaussians

Fe XIX (592.23A) - Short dashed

Fe XII (592.62A) – Long dashed

Milligan et al. ApJ 2006

Velocities from Line Profiles during a solar flare

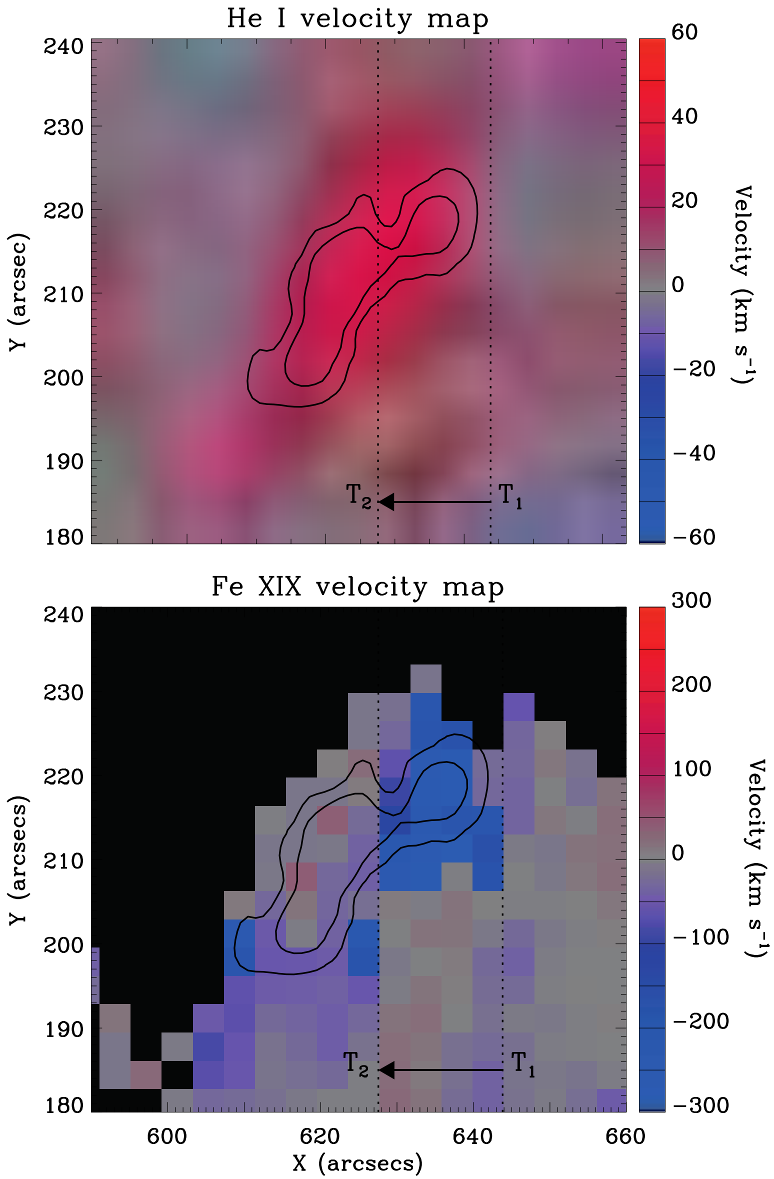

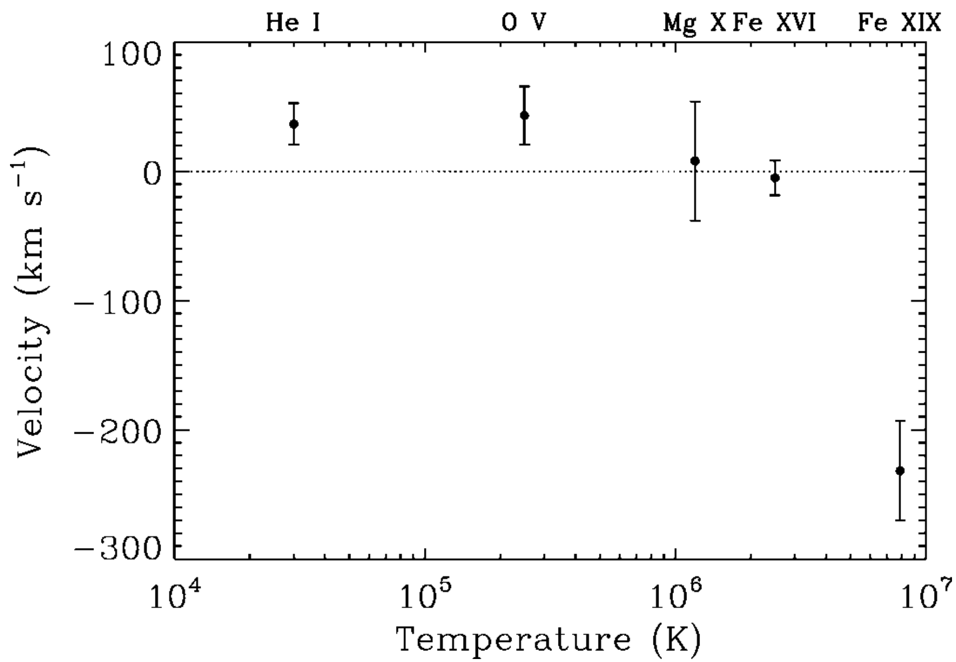

- Weak downflows in cooler lines (He I)
- Strong upflow in hot line (Fe XIX)

Chromospheric evaporation – Stellar Flare

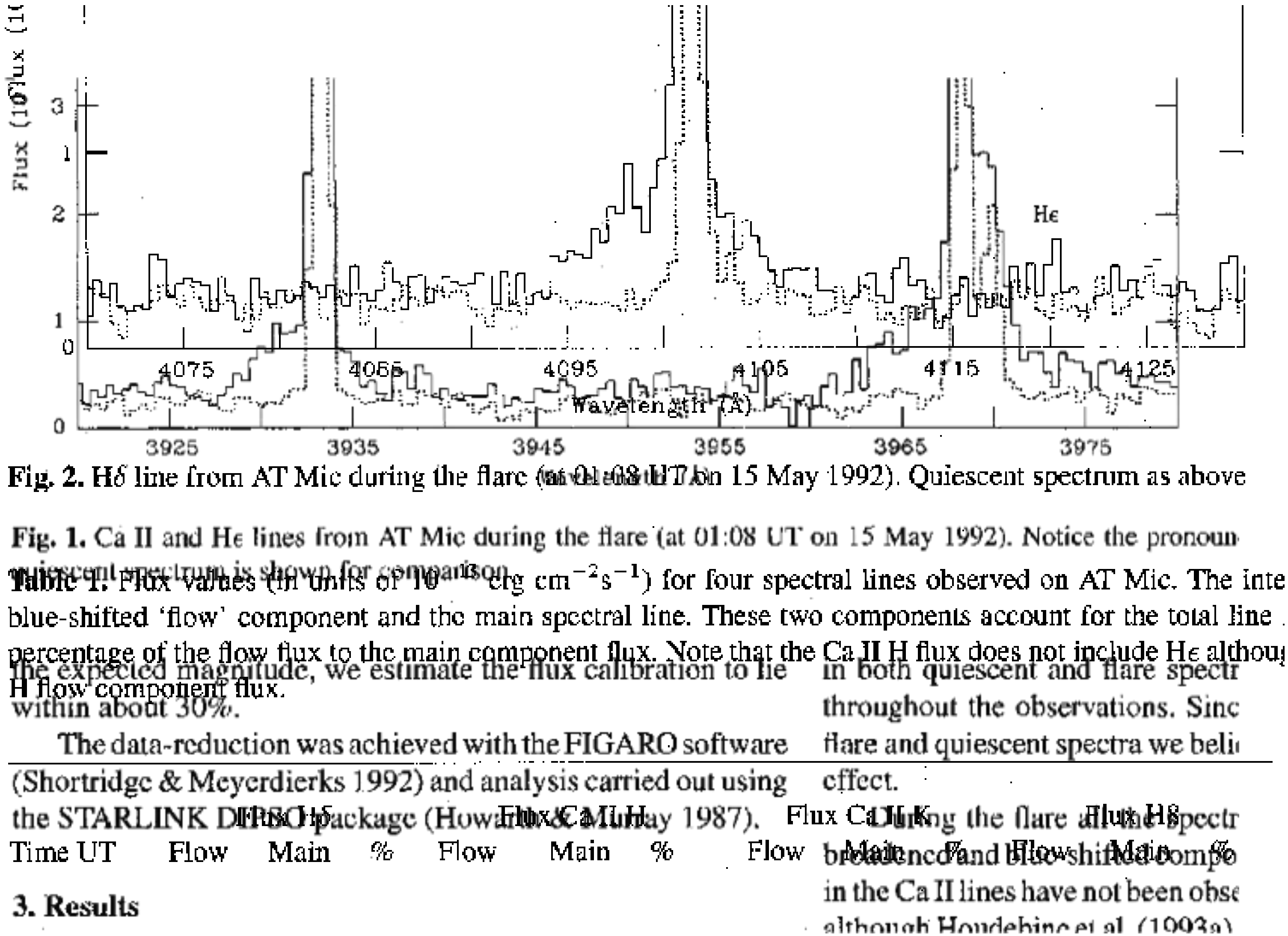

Velocities as high as 500 km/s

Bisectors & line asymmetries

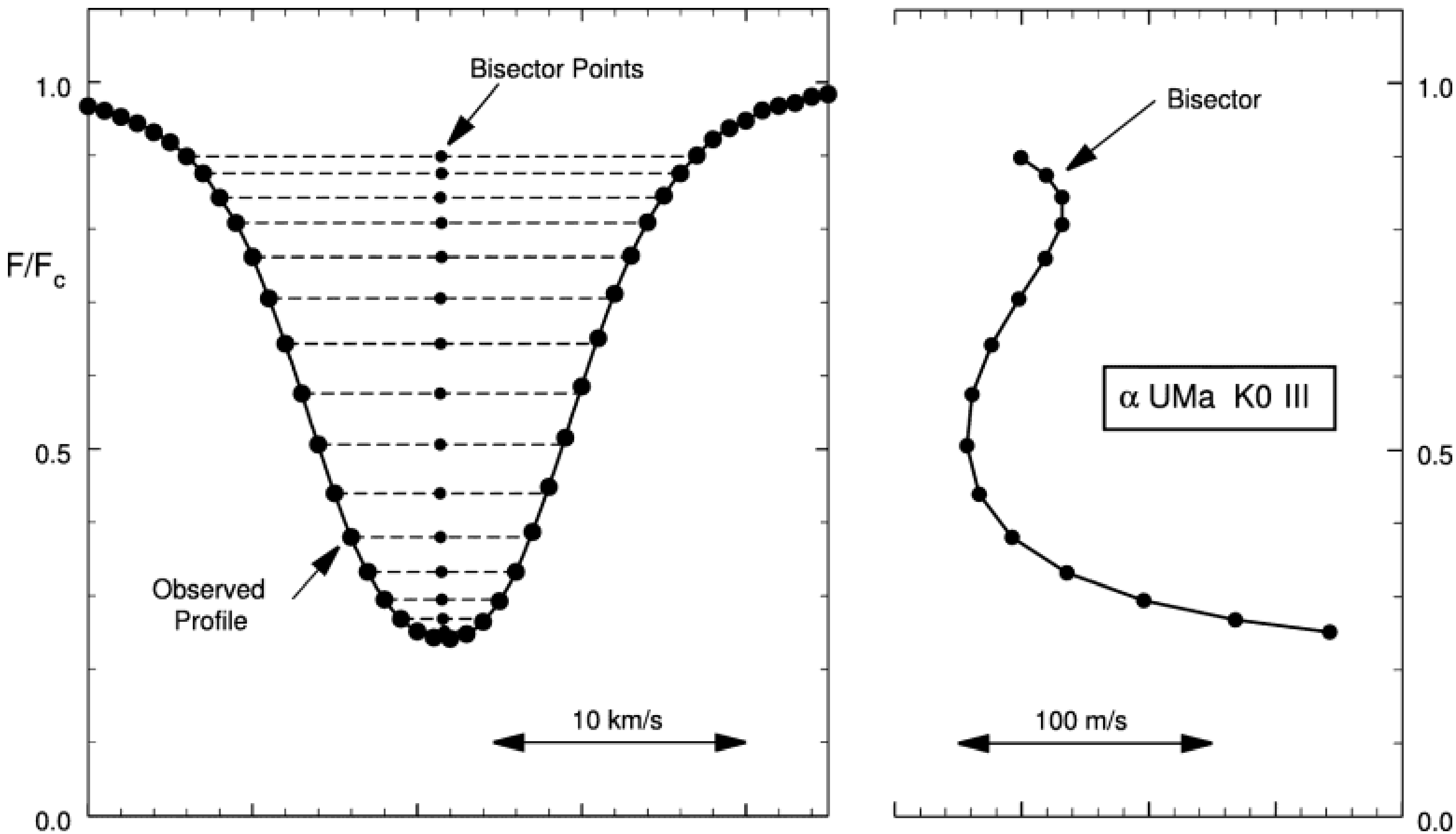

Horizontal line segments across the profile at equal intensities

Zooming in (right) shows a highly asymmetric profile

Velocities from line profiles during a solar flare

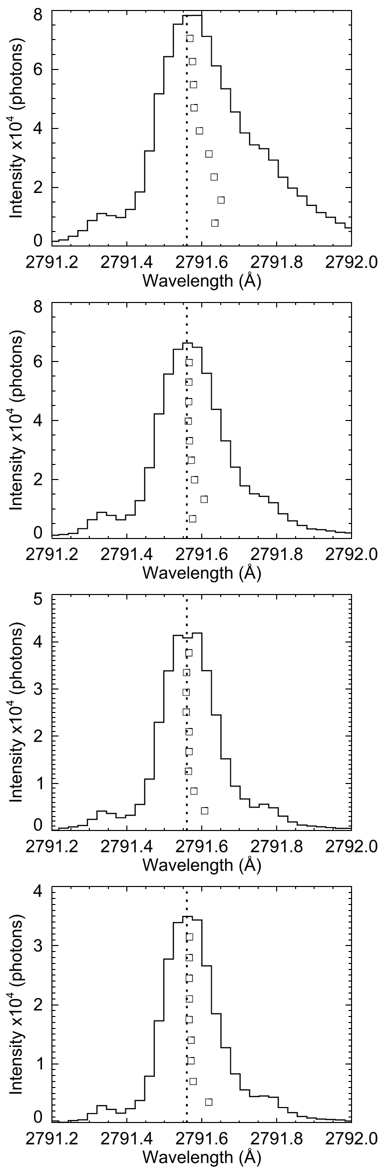

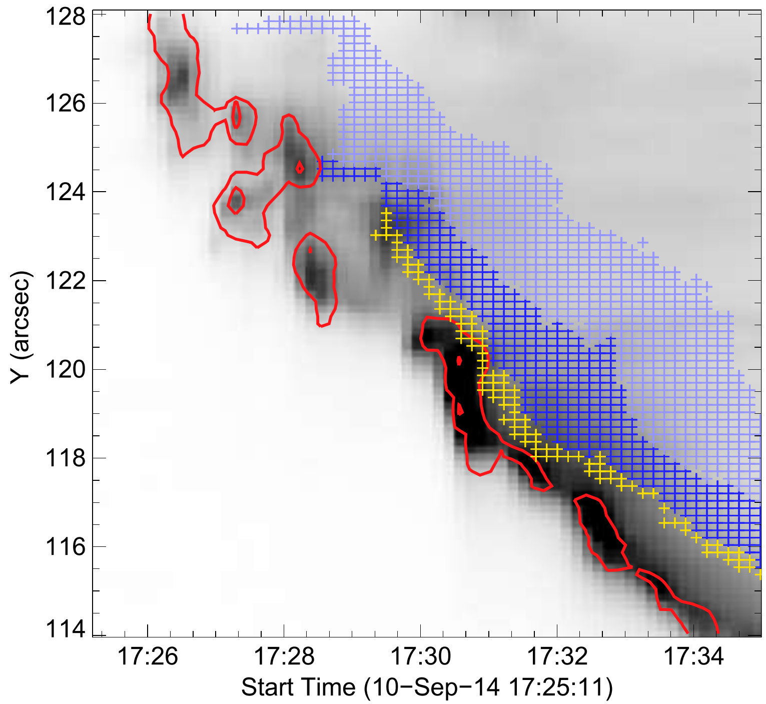

Graham & Cauzzi 2015

Electron Densities – Hydrogen Balmer

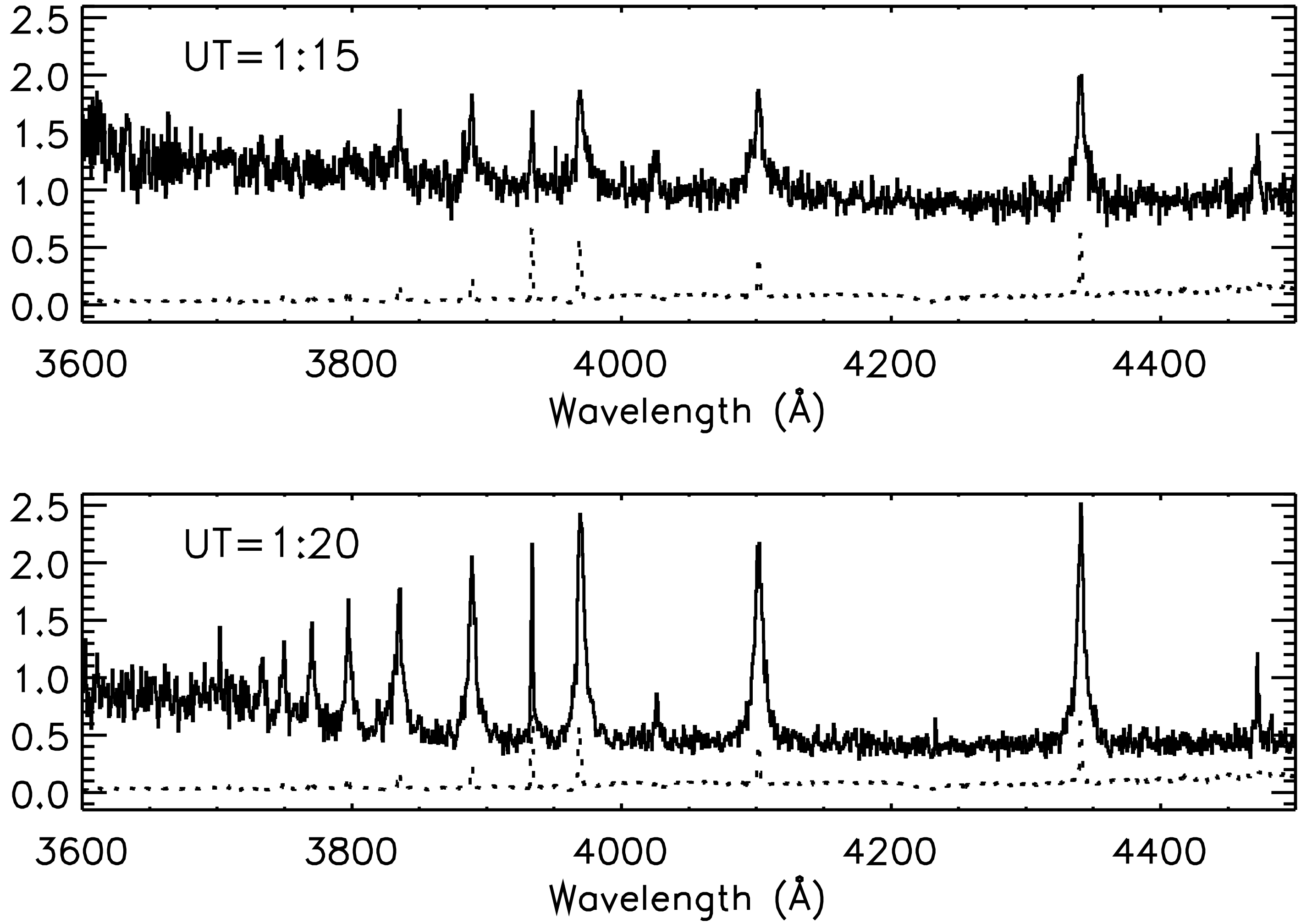

- Stark Broadening in Hydrogen Balmer lines
- Increased width of the outer wings – Ca II K remains unaffected
- Line core remains unaffected – No velocity shifts
- Electron densities of $5 \times 10^{13} - 10^{14}$ cm^{-3}

García-Alvarez et al. A&A 2002

Doppler velocities – Narrow band filters

- Construction of blue (λ – Δλ) and red (λ + Δλ) wing images.
- The intensity difference between the images provides a Doppler shift. In a symmetric profile there is no difference in intensity.

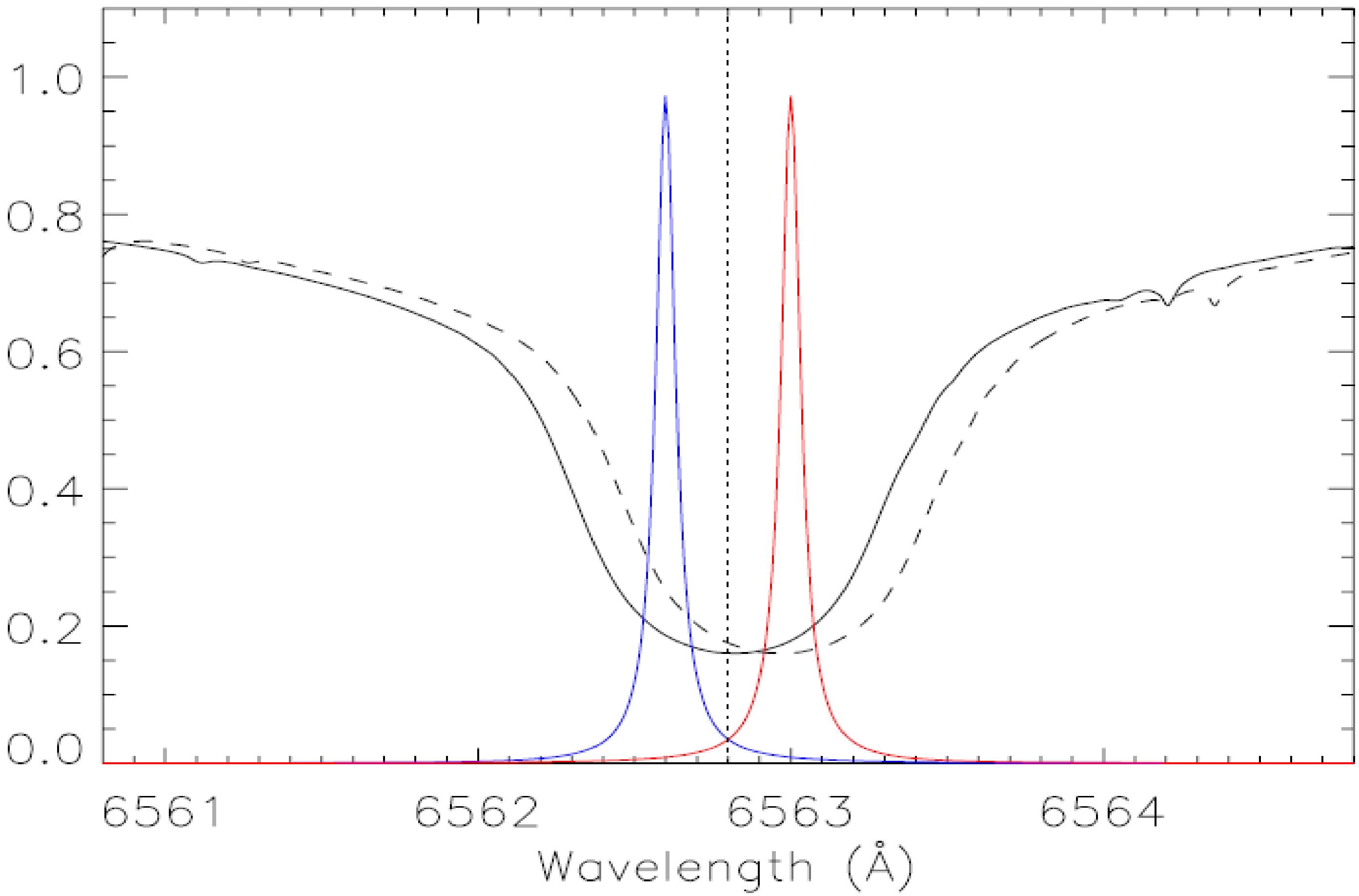

$\lambda_0 - 70$mA

$\lambda_0 - 35$mA

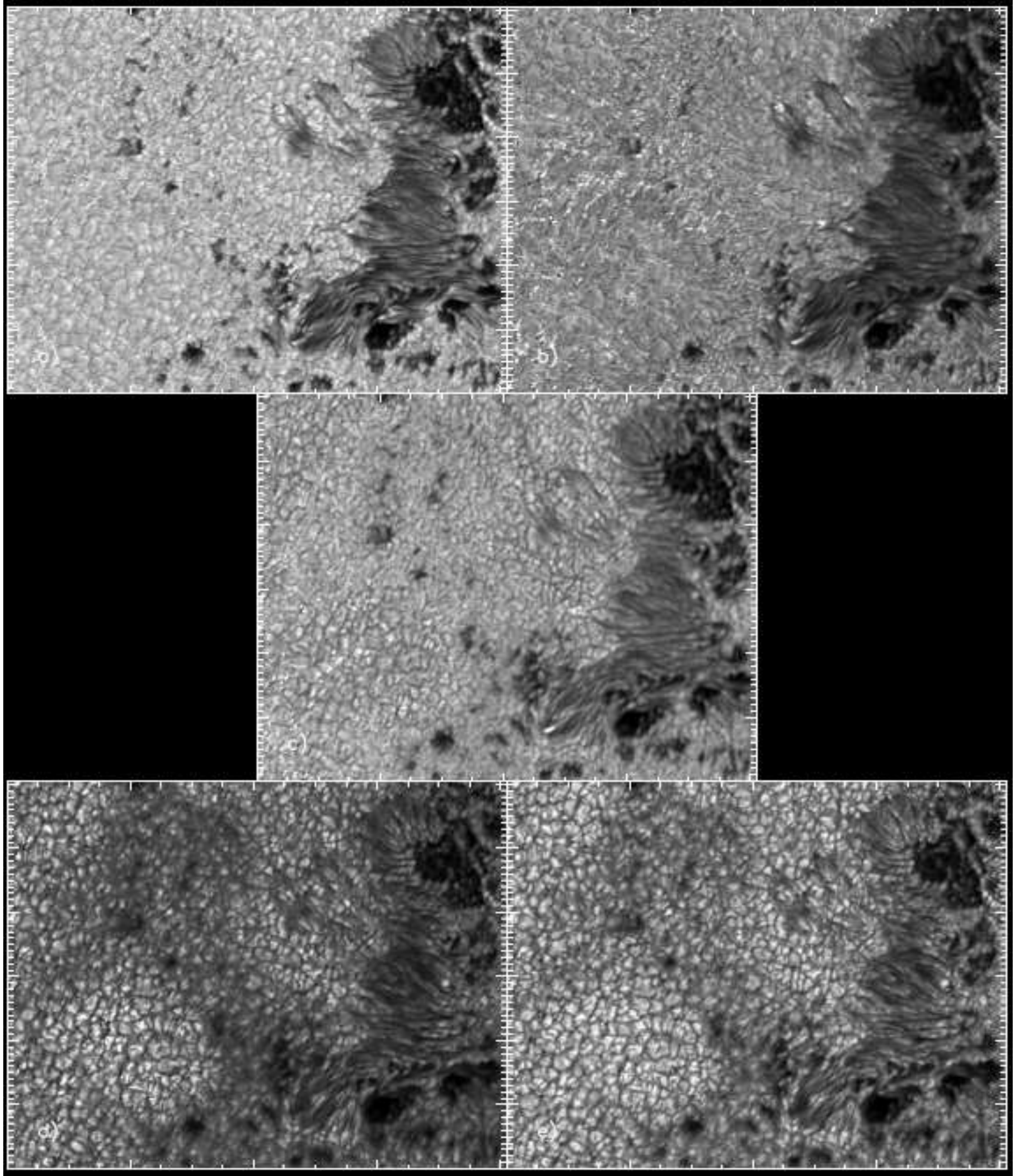

λ_0

$\lambda_0 +$ 35mA

$\lambda_0 +$ 70mA

Sutterlin et a

Magnetic Fields
Zeeman effect – Line broadening

- The degeneracy of an atomic level can be removed by the magnetic field
- $\Delta\lambda = 4.67 \times 10^{-13}\, g\, \lambda^2\, B_{//}$

  where $B_{//}$ is the line of sight component of B
- Select lines with similar atmospheric characteristics but different Lande g values
- Lines with high g values should be broader
- Method works well for red/infrared lines

  Method works well for strong fields

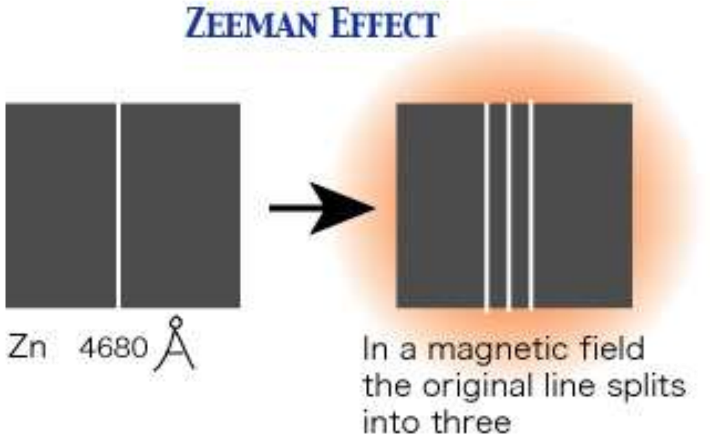

Magnetic Fields – WD

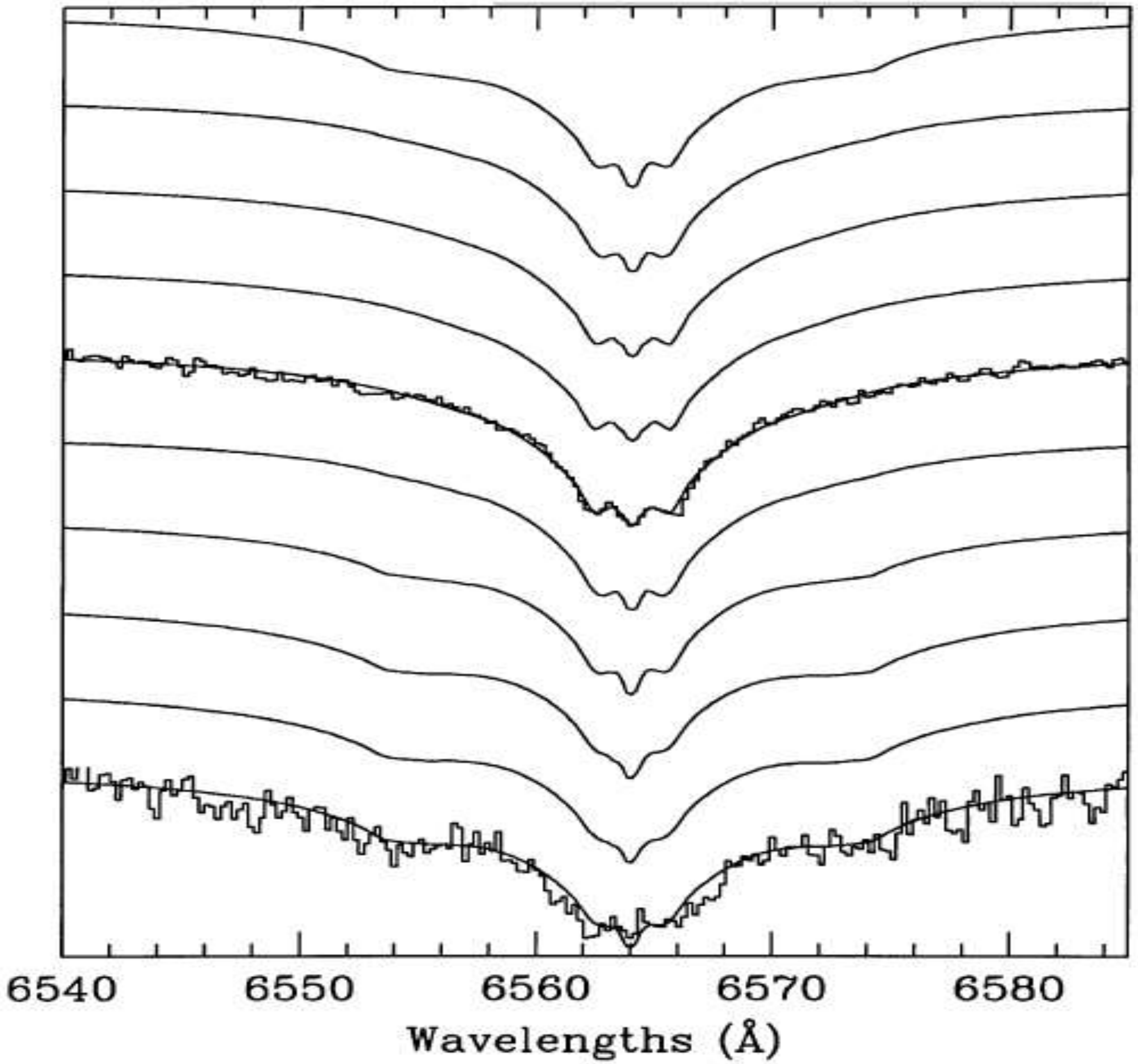

Maxted et al. (2000)

Polarization

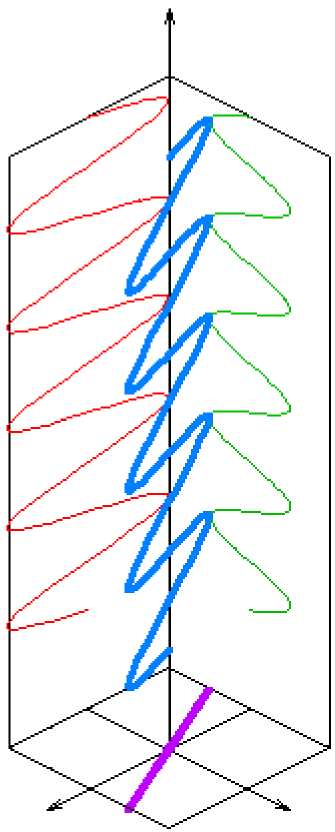

Linear
Vector has a constant direction

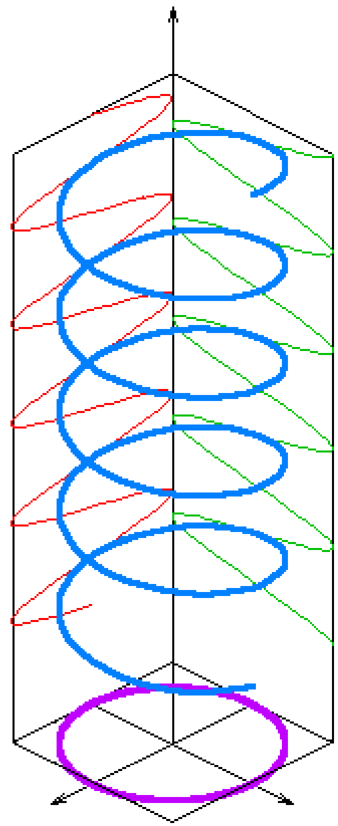

Circular
Vector rotates
Out of phase by 90°

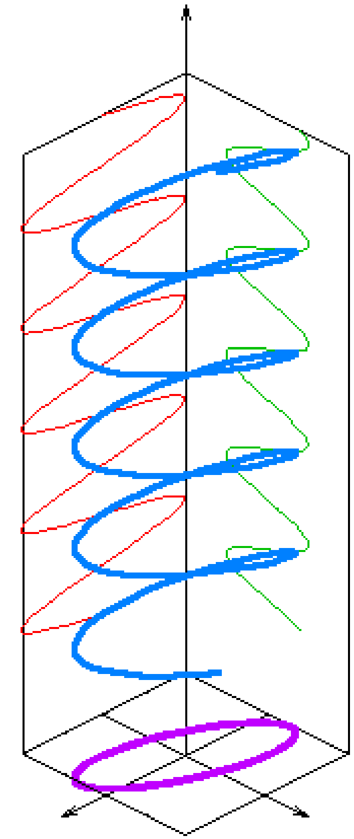

Elliptical
Vector magnitude varies
Out of phase

Magnetic Fields
Zeeman effect – Polarization

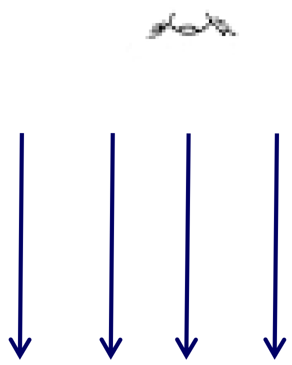

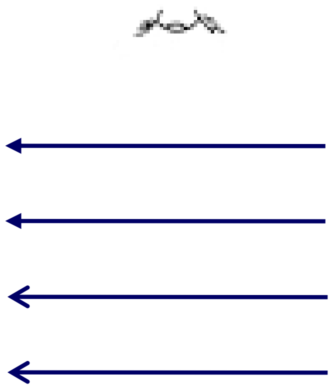

- **Longitudinal case**

B ∕∕ to the line of sight

- **Transverse case**

B ⊥ to the line of sight

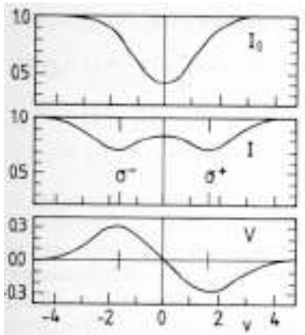

- **Splitting proportional to the magnetic field**
- **Components are polarized**

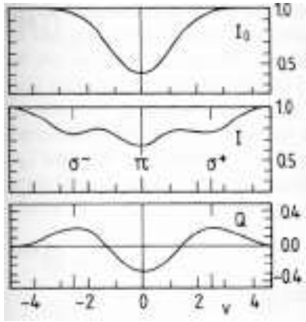

Stokes parameters
Phase and polarization of the radiation

Radiation propagating along the z axis.

E field lies in the x-y plane :

$E_x = E_{0x} \cos(2\pi\nu t)$ $E_y = E_{0y}\cos(2\pi\nu t + \delta)$

I - intensity	$I = E_{0x}^2 + E_{0y}^2 = I_u + I_p$
Q - linear	$Q = E_{0x}^2 - E_{0y}^2$
U - linear ($\pm$ 45°)	$U = 2E_{0x}E_{0y}\cos\delta$
V - circular	$V = 2E_{0x}E_{0y}\sin\delta$

Stokes parameters
Phase and polarization of the radiation

- $V = 0.5\,[I(\lambda - \Delta\lambda) - I(\lambda + \Delta\lambda)]$

$$\Delta\lambda = 4.67 \times 10^{-13}\, g\, \lambda^2\, B_{//}$$

$B_{//} = C \times V/I$ (LOS component of B)

- $Q = 0.5\,[-I(\lambda) + 0.5[I(\lambda + \Delta\lambda) + I(\lambda - \Delta\lambda)]\,]$

$$B_{\perp} = D \times [(Q/I)^2 + (U/I)^2]^{0.25}$$

$B_{\perp} = D \times (Q/I)0.5$ (for $U = 0$)

where C, D depend on the g value of the line

$\theta = \tan^{-1}(B_{\perp} / B_{//})$ $\psi = 0.5 \tan^{-1}(U/Q)$

Ronan et al. (1987)

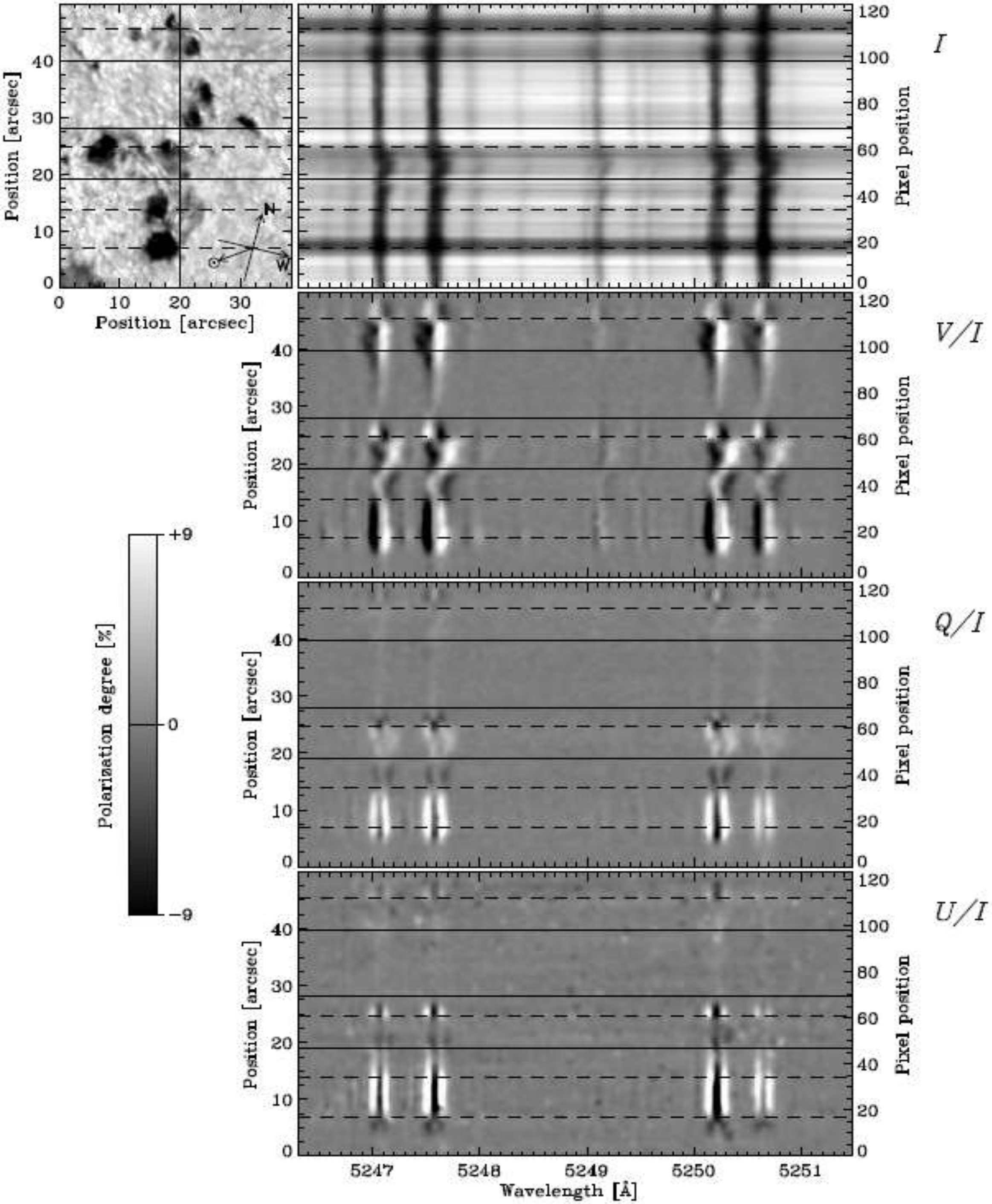

An example

- Stokes profiles of NOAO 7500
- Fe I lines around 5250A
- ZIMPOL I, SVTT
- λ / Δλ = 175,000

Bernasconi et al. (1998)

An example (cont)

- Stokes profiles of NOAO 7500 – pixel position 21
  - Fe I lines

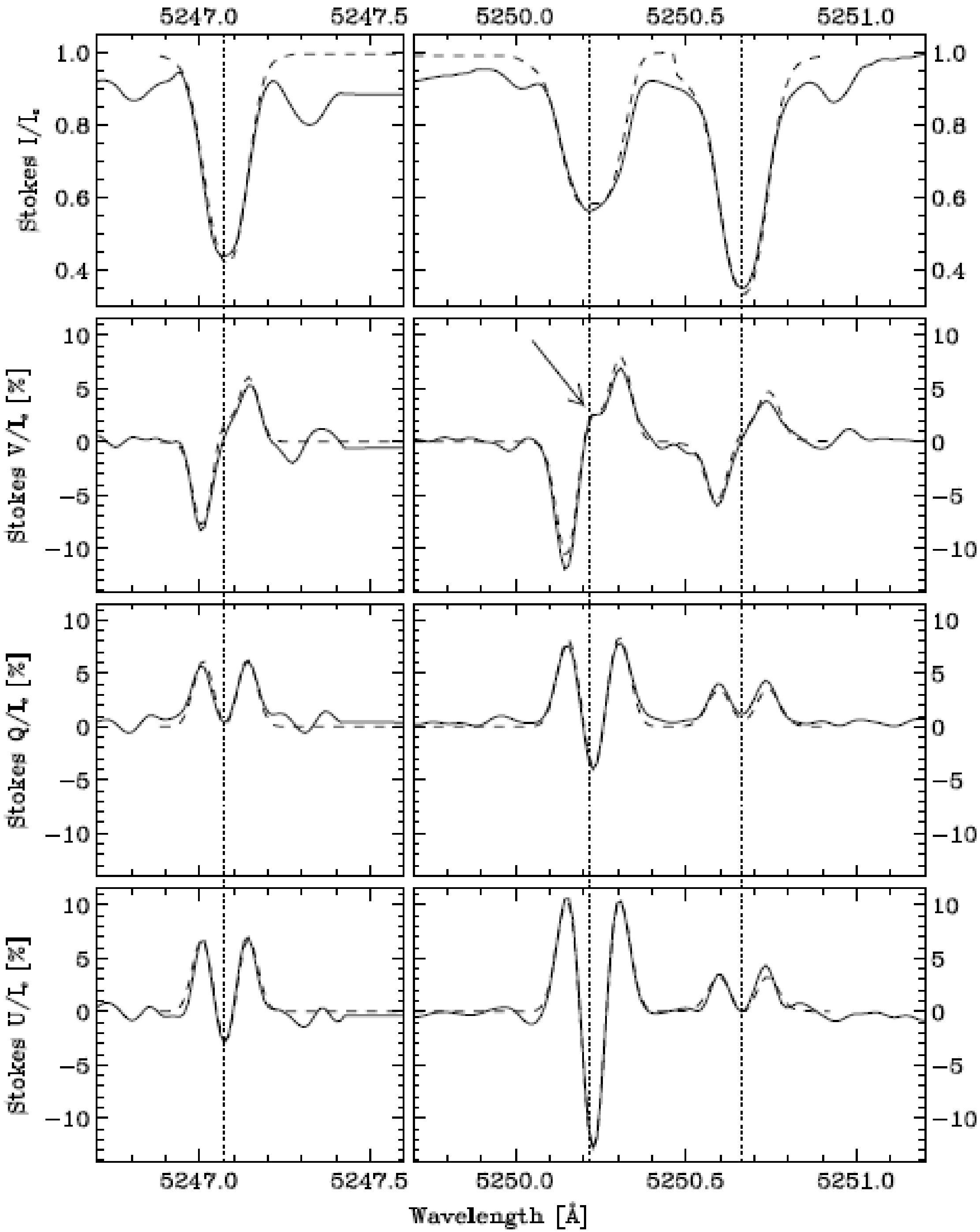

Bernasconi et al. (1998)

Spectral resolution

- $\Delta\lambda$ (given in A or nm)

  The lower the $\Delta\lambda$ the higher the resolution

- $R = \lambda / \Delta\lambda$ (dimensionless) –
- $v / c = \Delta\lambda / \lambda$

  The higher the R the higher the resolution the lower

  the velocities we can accurately measure

  Spectral resolution depends on :

- Slit width (has to stay smaller than the resolution element)
- Detector pixel size (at least 2 pixels per resolution element)

  (sampling theorem)

- Optics

Grating spectroscopy

- Grating equation

$$n\,\lambda = d \sin\theta$$

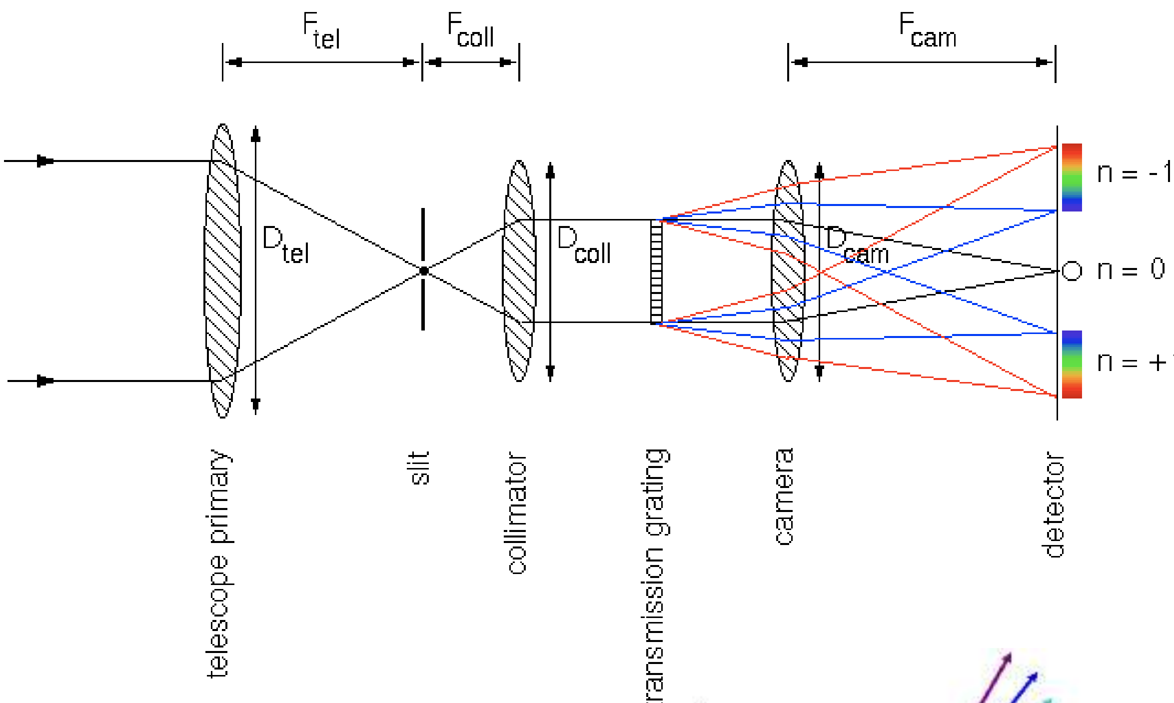

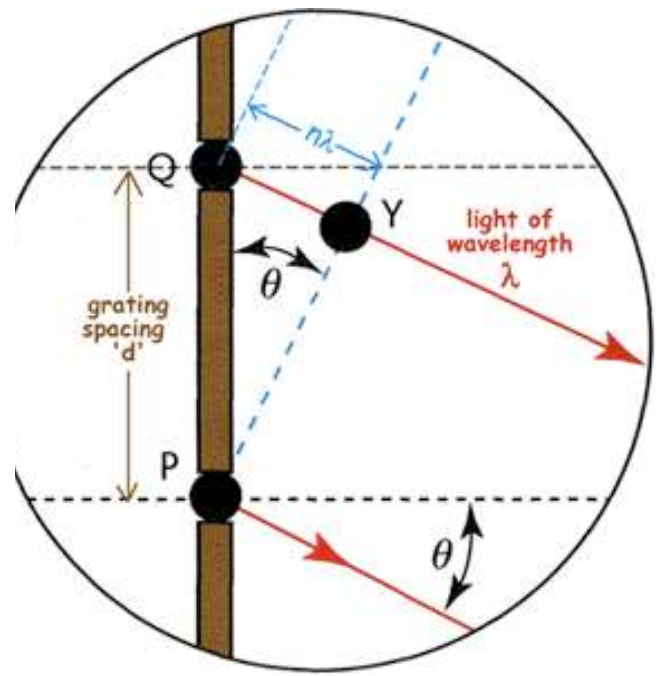

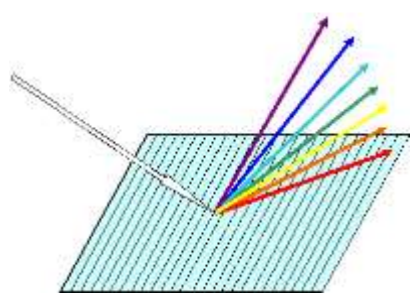

Imaging Spectroscopy (slit based)

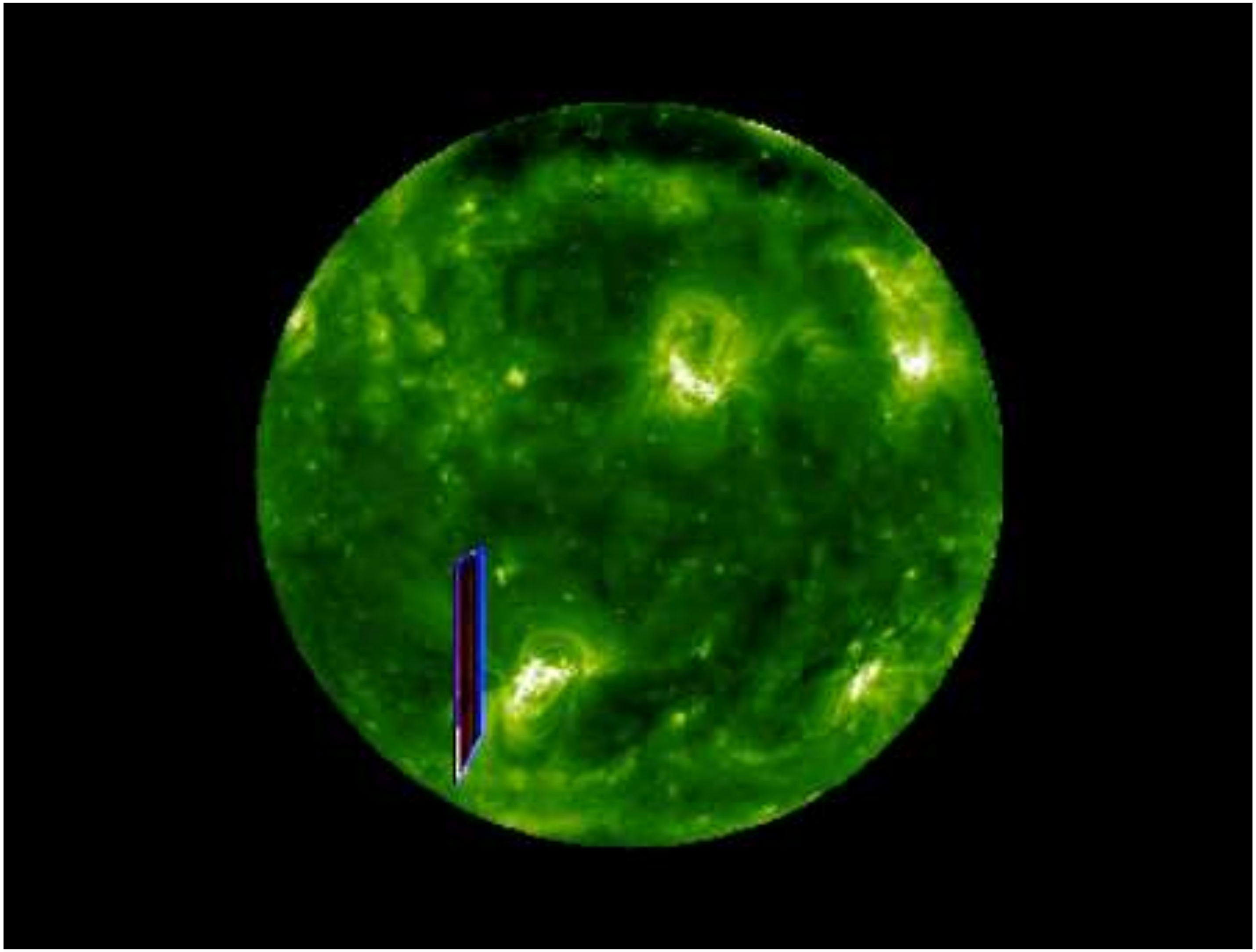

- A full spectrum is obtained in each slit position
- The slit must raster for imaging spectroscopy (low temp resolution)
- Very good wavelength coverage

Credit: MSSL

Doppler velocities - Fabry-Perot Interferometer

- An arrangement of two partially reflecting surfaces (**etalon**) (high reflectance – very low absorption)
- Pairs of rays differ in their path length by $\Delta P = 2\, d \cos\theta$
- Constructive interference for $n\, \Delta P = m\, \lambda$ (m an integer)
- Image formed for wavelengths $\lambda = 2\, d\, n \cos\theta / m$
- Select wavelength by adjusting *d, n*, or θ (tune the etalon)

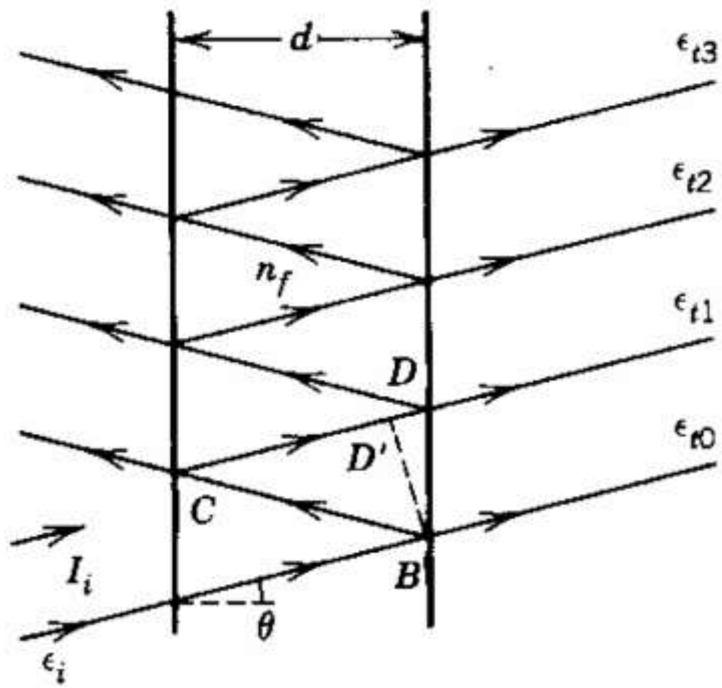

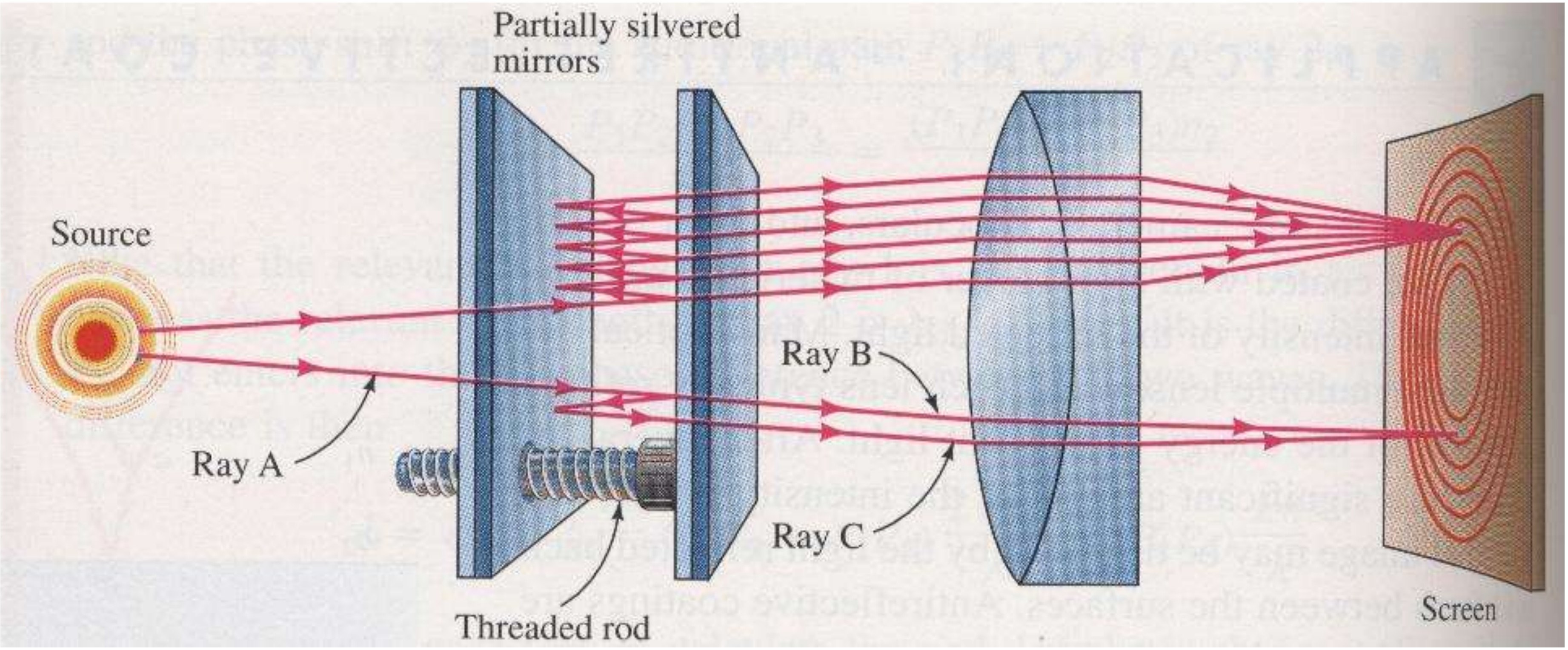

$$\lambda = 2\, d\, n\, \cos\theta / m$$

Imaging Spectroscopy (Fabry-Perot)

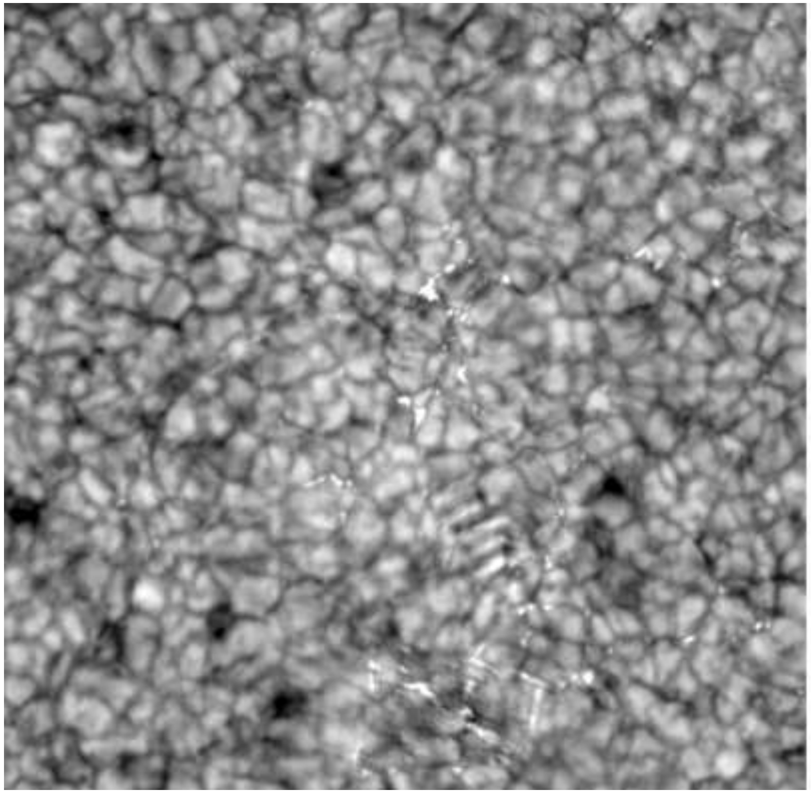

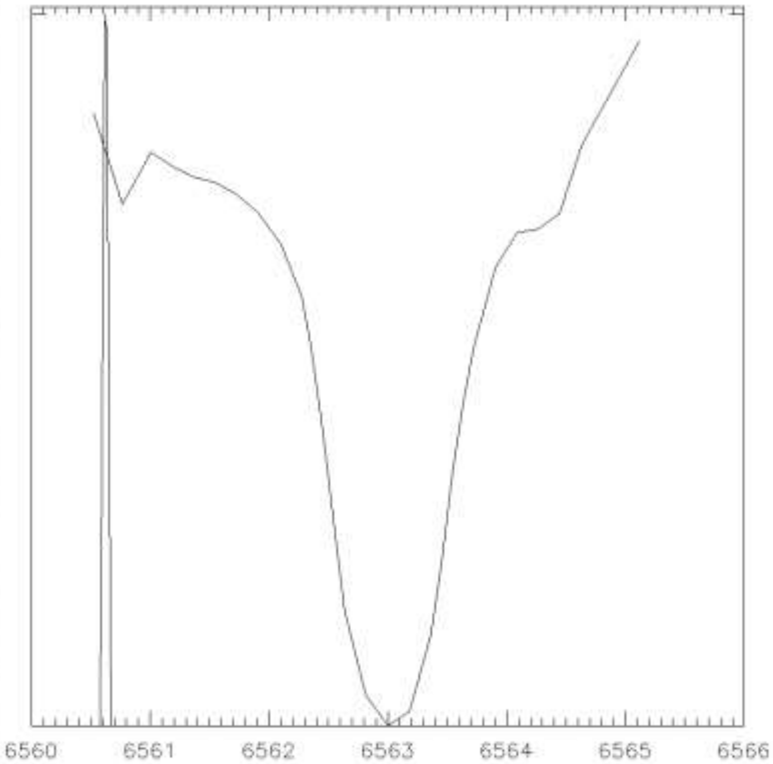

- The full fov is obtained in a single wavelength position
- The FP in tuned in the wavelength domain to construct the line profile
- Very high temporal resolution (sub-sec)
- Poor wavelength coverage (a few A) – Good for single lines

Activity Cycles - Spectroscopy
The Mount Wislon S index

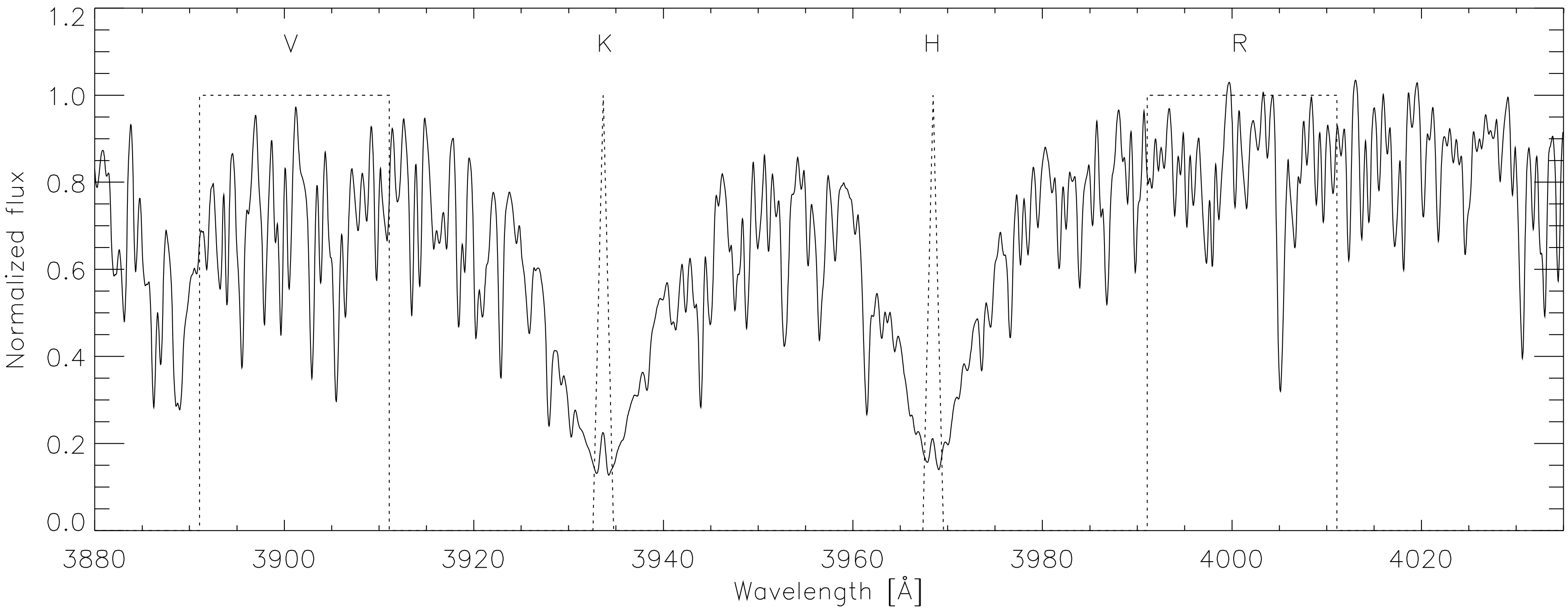

S index based on the Ca II H&K lines

$$S_{MWO} = (N_H+N_K) / (N_R+N_V)$$

Vaughan et al. 1978

Activity Cycles

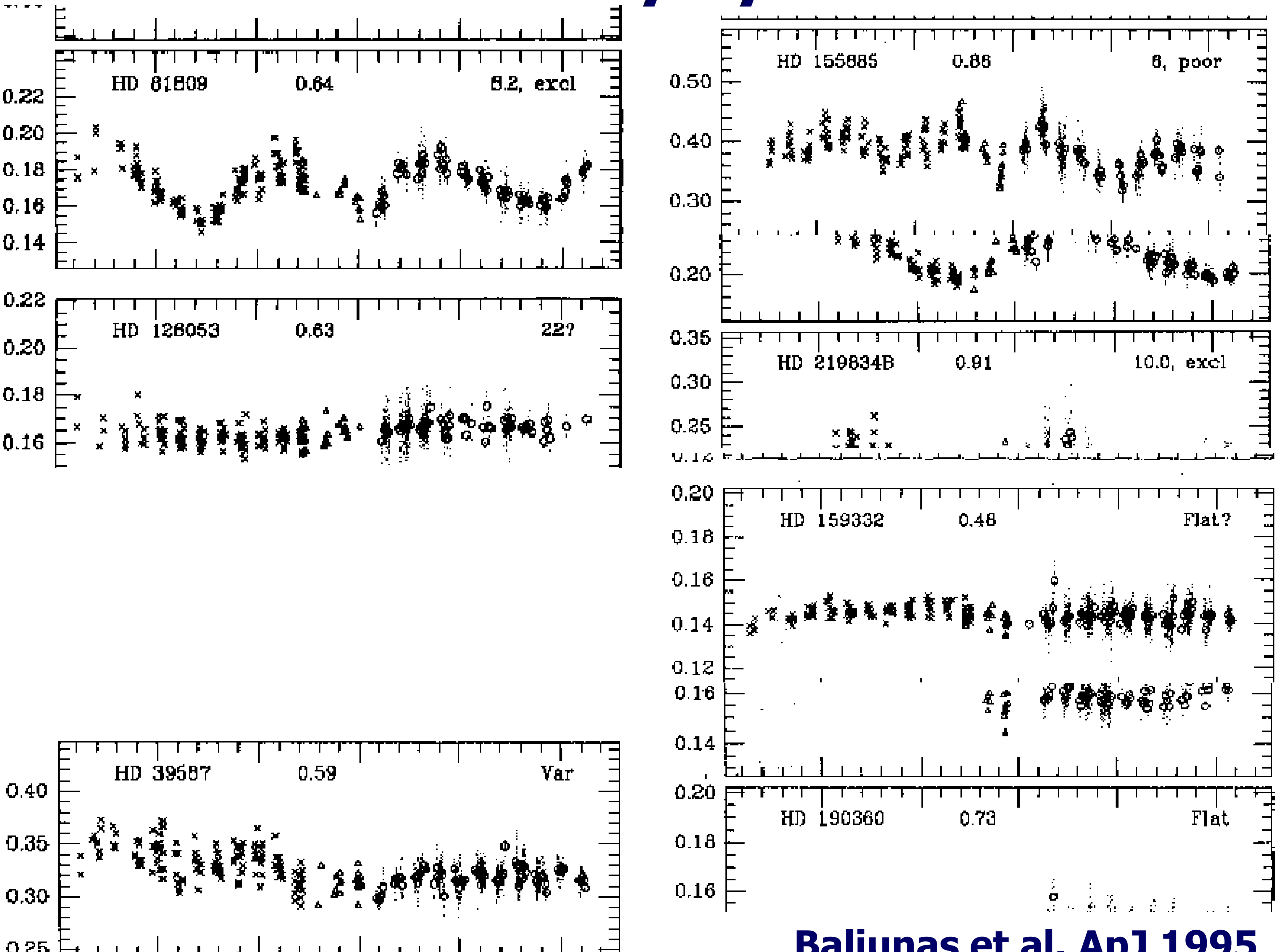

Baliunas et al. ApJ 1995

EUV Spectroscopy

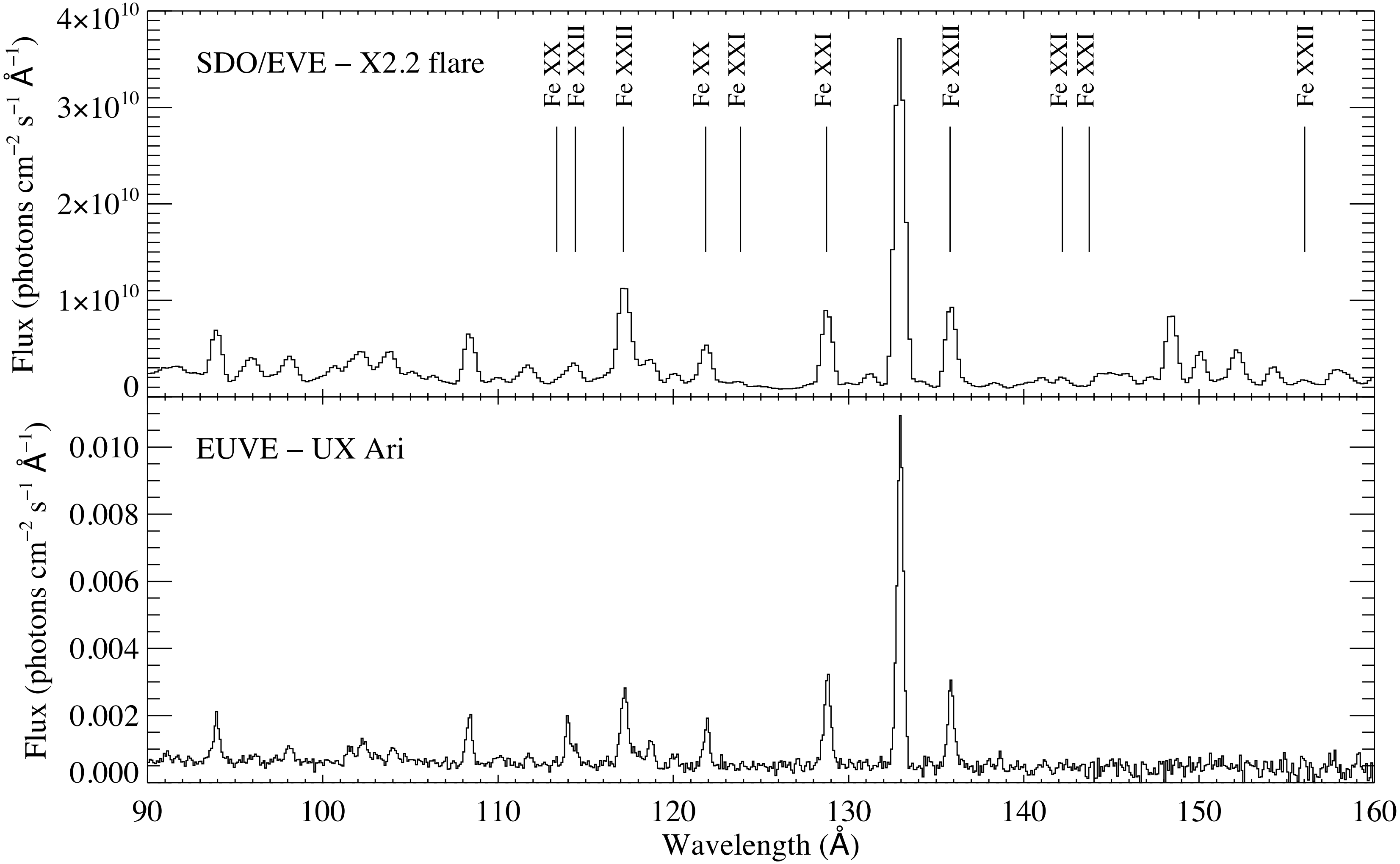

Comparison of X2.2 with UX Ari in quiescent – Identical spectra

Daniel K. Inouye Solar Telescope

- The 4m DKIST on Haleakala, HI will be the world's largest solar telescope and the premier facility for solar research!
- The construction and operations of DKIST are funded primarily by the National Science Foundation, with partner contributions from Germany and UK.